Journal of Multidisciplinary Engineering Science Studies (JMESS)
ISSN: 2458-925X
Vol. 6 Issue 5, May - 2020

Effects Of Multiple Reflections Of Light Within An Equilateral Prism

Antonio Parretta[1,2]
[1]Physics and Earth Science Department,
Ferrara University, Via Saragat 1, 44122 Ferrara, Italy.
parretta@fe.infn.it
[2]Academy of Sciences of Ferrara,
Palazzo Tibertelli, Via del Gregorio 13, 44121 Ferrara, Italy.
aparretta@alice.it

***Abstract*— By illuminating an equilateral prism with white light, the light internally refracted, besides being refracted externally giving rise to the well-known spectrally dispersed beam, is internally reflected an indefinite number of times also producing an indefinite number of externally refracted beams. An external refracted beam can be white or spectrally dispersed depending on the parity of the number of internal reflections undergone. After a brief introduction to recall the main concepts at the basis of the use of the prism as light dispersing element, I analyze, both theoretically and experimentally, the properties of the light beams exiting the faces of the equilateral prism, when it is illuminated with a laser beam, or with a white light beam, polarized "*p*", "*s*" or unpolarized.**

Keywords—equilateral prism, multiple internal reflections, white light, dispersed light

I. INTRODUCTION

It is well known that the rainbow phenomenon, with its various orders, occurs as a consequence of the multiple reflections of light inside the water droplets [1-9]. Something similar happens in the equilateral prism, although not the same due to its triangular geometry compared to the spherical one of water droplets. In fact, by appropriately orienting the prism with respect to a beam of white light at the entrance, one can observe, from each face, a series of alternately white and dispersed beams, which depend on the number of internal reflections undergone by the input light before being refracted at the exit. Before tackling the study of multiple internal reflections in an equilateral prism, however, it is useful to briefly review some concepts at the basis of the traditional use of the prism as a white-light spectrally dispersing optical element [10-21]. To this end, the method used to measure the refraction index of the prism will be reviewed and soon after the exit angles of rays will be studied as a function of the angle of the entry light and of its wavelength. Subsequently, the symmetrical path inside the prism of a monochromatic light beam will be analyzed and its intensity calculated at each interaction with the glass/air interface, recalling the fundamental Fresnel equations for "*p*" or "*s*" polarized light. This study will then be extended to white light and the spectral transmissions of the main refracted beams will be calculated, always distinguishing between "*p*" and "*s*" polarization. The theoretical analysis done with monochromatic light will be accompanied by some experimental measurements of intensity of a laser beam, while that made with white light will be accompanied by some visualizations of the refracted light beams at the exit of the prism.

II. MEASUREMENT OF THE REFRACTION INDEX AND DEFINITION OF THE MAIN OPTICAL QUANTITIES

A. Symmetrical path of a monochromatic light beam

Let us consider a generic prism with opening angle α, and refractive index $n(\lambda)$ to be determined (see Fig. 1). The simplest and most immediate way to measure the refraction index of the prism glass as a function of the wavelength is to illuminate it with a parallel beam of monochromatic light, oriented with respect to the prism so as to have a symmetrical path, as illustrated in fig. 1. It is also possible to use white light at the input, provided that the wavelength corresponding to a symmetrical path of the light is selected on the face (2). We will have, therefore, that the angle of incidence on the face (1) will be equal to that of refraction on the face (2): $\beta(\lambda) = \beta'(\lambda)$. We call with γ and χ the angles of the isosceles triangle formed inside the prism with the normals to faces (1) and (2), and with the light path (Fig. 1). In these conditions, the incoming and exiting rays will form the same angle ($\beta - \gamma$) with respect to the horizontal line.

The refractive index $n(\lambda)$ can be obtained starting from the quantities α, β and λ applying the Snell's law:

$$\gamma = \pi/2 - (\pi - \alpha)/2 = \alpha/2 \quad (1)$$

$$\chi = \pi - 2\gamma = \pi - \alpha \quad (2)$$

$$n(\lambda) = \sin[\beta(\lambda)] / \sin\gamma = \sin[\beta(\lambda)] / \sin(\alpha/2) \quad (3)$$

In these conditions, the incident ray, after refraction, undergoes a deviation in the clockwise direction equal to:

$$\Delta(\lambda) = 2[\beta(\lambda) - \gamma] = 2\beta(\lambda) - \alpha \quad (4)$$

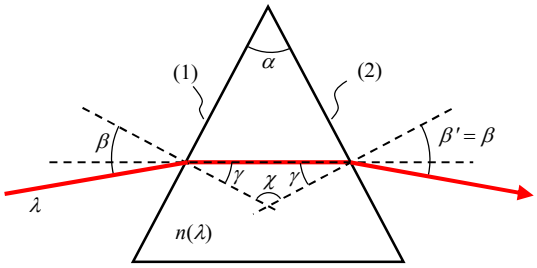

fig. 1. Section of the prism, illuminated on face (1) with a beam having the same angle of entry and exit.

If instead of a generic prism we use an equilateral prism ($\alpha = \pi/3$), Eqs. (3) and (4) simplify:

$$n(\lambda) = \{\sin[\beta(\lambda)] / \sin(\pi/6)\} = 2\sin[\beta(\lambda)] \quad (3')$$

$$\Delta(\lambda) = 2[\beta(\lambda) - (\pi/6)] = 2\beta(\lambda) - \pi/3 \quad (4')$$

The refractive index $n(\lambda)$ can be obtained also by setting a different angle of incidence; in this case the formulas are slightly more complicated and will be shown in the next section.

Let us now consider an equilateral prism and a ray of monochromatic light (see the continuous green line in Fig. 2) incident at point A, centered on the side (1) of the optical section, and refracted along the direction parallel to the base side of the prism. In these conditions, on side (2) of the prism optical section and in the central point B, in addition to the refracted component (continuous green line), there will be an internally reflected component (dashed green line) incident on point C of side (3), then on point A of side (1), and finally on point B of side (2), where it will give rise to a secondary refracted beam (dashed green line) which will overlap the primary refracted beam. As the internally reflected beam (dashed green) undergoes three more reflections than the primary refracted beam, it will be much less intense.

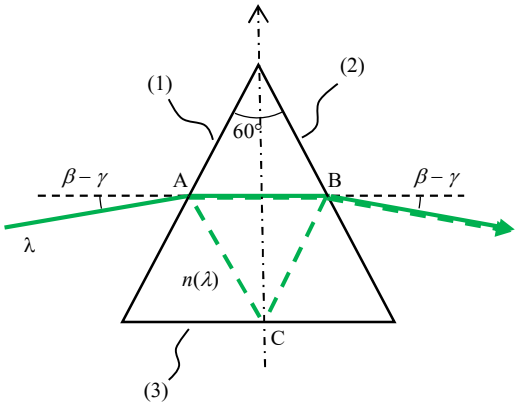

fig. 2. The primary beam is reflected three times within the prism before being refracted externally (dashed green line), overlapping the previously refracted component (continuous green line).

To observe this secondary beam, we can "decouple" it from the primary one changing the incidence point on side (1), as shown in Fig. 3. In the following we will call "secondary beams" all those beams that arise from reflections inside the prism, and "primary beams" the incident one, the one reflected in the air and that refracted without internal reflections.

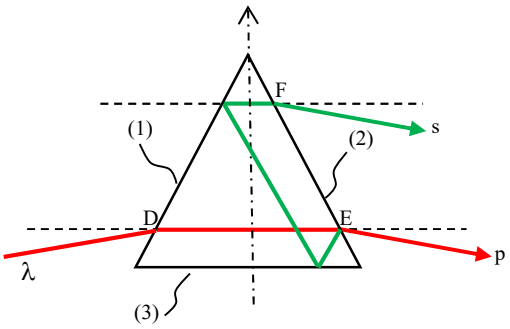

fig. 3. The prism is illuminated by a light beam incident away from the center of face (1).

The primary beam (p) exits from point E and the secondary beam (s) from point F, being directed along the same direction. The points E and F are equidistant from the center of the side (2); projecting the beams (p) and (s) on a screen, they can be observed separately.

B. Input Beam with Generic Angle of Incidence

Let us analyze now the behavior of the prism when the incoming ray is incident at a generic angle β, but always within the limits allowed by the appearance of a primary refracted beam out of the prism (see Fig. 4).

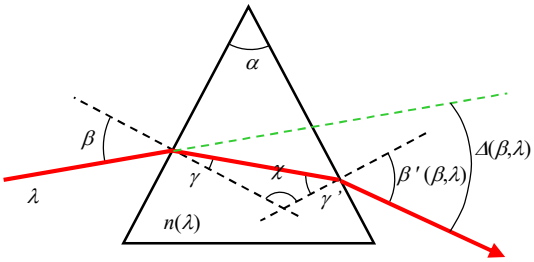

fig. 4. The prism is illuminated by a light beam incident on face (1) at a generic angle β.

Let us now calculate $\Delta(\lambda)$ knowing: α, β, $n(\lambda)$. First of all, we note that the angle χ given by Eq. (2) does not depend on the position of the two normals to faces (1) e (2), so we have for the total deviation of the ray (see Fig. 4):

$$\Delta(\lambda) = (\beta - \gamma) + (\beta' - \gamma') \quad (5)$$

$$\gamma' = \pi - \chi - \gamma = \pi - (\pi - \alpha) - \gamma = \alpha - \gamma \quad (6)$$

$$\Delta(\lambda) = \beta - \gamma + \beta' - \alpha + \gamma = \beta + \beta' - \alpha \quad (5')$$

But the exit angle of the beam is obtained from Snell's law:

$$\sin\beta' = n \cdot \sin\gamma' = n \cdot \sin(\alpha - \gamma) = \ldots$$

$$\ldots = n \cdot \sin[\alpha - \sin^{-1}(\sin\beta / n)] \quad (7)$$

$$\beta' = \sin^{-1}\{n \cdot \sin[\alpha - \sin^{-1}(\sin\beta / n)]\} \quad (8)$$

From Eqs. (5') and (8) we finally obtain:

$$\Delta(\lambda) = \beta - \alpha + \sin^{-1}\{n(\lambda) \cdot \sin[\alpha - \sin^{-1}(\sin\beta / n(\lambda))]\} \quad (9)$$

Eqs. (8) and (9) are the fundamental formulas telling us how the prism works at the different wavelengths. Let us now ask what should be the angle of incidence β to have at the exit an angle of refraction $\beta' = \beta$, or, equivalently, to have a ray path inside the prism parallel to side (3). It must be:

$$\beta = \beta' = \sin^{-1}\{n \cdot \sin[\alpha - \sin^{-1}(\sin\beta / n)]\} \quad (10)$$

$$\sin\beta / n = \sin[\alpha - \sin^{-1}(\sin\beta / n)] \quad (10')$$

Solving Eq. (10') for $\sin\beta / n$, we finally obtain:

$$\sin\beta = n \cdot \sin(\alpha / 2) \quad (11)$$

In this way, knowing α and $n(\lambda)$, β will be a function of λ given by:

$$\beta(\lambda) = \sin^{-1}[n(\lambda) \cdot \sin(\alpha / 2)] \quad (12)$$

For an equilateral prism, ($\alpha = 60°$), we have:

$$\beta(\lambda) = \sin^{-1}[n(\lambda) / 2)] \quad (12')$$

Let us now apply what found so far using a SCHOTT's N-SF11 prism. We derive the following dispersion formula (where λ is expressed in μm) [22]:

$$n^2 - 1 = [(1.73759695 \cdot \lambda^2) / (\lambda^2 - 0.013188707)] + \ldots$$
$$\ldots + [(0.313747346 \cdot \lambda^2) / (\lambda^2 - 0.0623068142)] + \ldots$$
$$\ldots + [(1.89878101 \cdot \lambda^2) / (\lambda^2 - 155.23629)] \quad (13)$$

For the wavelengths generally used with He-Ne lasers, we have:

$$n(\lambda_1) = n(532\ \text{nm}) = 1.7948\ (\text{green}) \quad (13')$$

$$n(\lambda_2) = n(633\ \text{nm}) = 1.7786\ (\text{red}) \quad (13'')$$

Fig. 5 shows $n(\lambda)$ in the 400-700 nm interval. Fig. 6 shows $\beta(\lambda)$ and $\Delta(\lambda)$ when the condition $\beta = \beta'$ is applied. Since the refractive index increases with decreasing wavelength, it is clear that the angle of incidence β must increase as the wavelength decreases to keep the condition $\beta = \beta'$. Notice how, according to Eq. (4), the angular excursion over the entire Vis of the angular deviation $\Delta(\lambda)$ (between ~65° and ~75°) is double that of the exit angle $\beta'(\lambda)$ (between ~62° and ~67°).

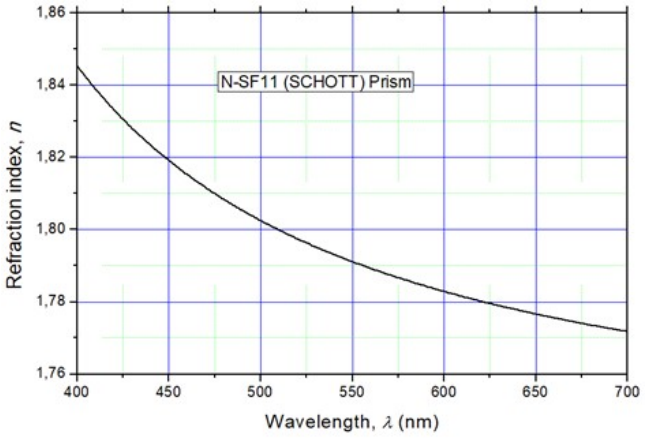

fig. 5. Refractive index of the N-SF11 glass.

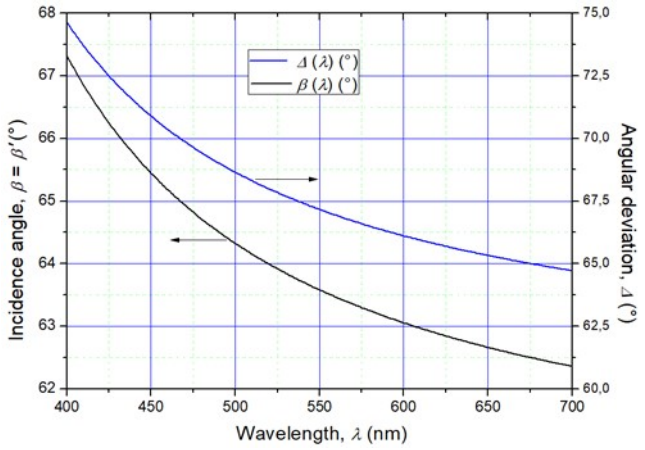

fig. 6. Wavelength dependence of incidence angle $\beta(\lambda)$ and angular deviation $\Delta(\lambda)$, when the condition $\beta = \beta'$ is applied.

Let us now consider a generic angle of incidence β. Fig. 7 shows the trend of the exit angle β' as a function of the input angle β, calculated for some Vis wavelengths: λ = 400, 450, 532, 633 and 700 nm, being the wavelengths λ = 532 and 633 nm chosen because used in the experiments. It is interesting to note that the incidence angle β shows a lower limit, ranging from ~50° to ~57° depending on the wavelength, due to the appearance of the total internal reflection (TIR) phenomenon at face (2) of the prism [23]. In correspondence with this limit, the exit angle β' reaches 90° and then it is not possible to further decrease the angle β without cancelling the light refracted externally. For the same Vis wavelengths, Fig. 8 shows the trend of the total angular deviation Δ as a function of the angle β. While the exit angle β' grows monotonously as the entry angle β decreases, the total angular deviation Δ shows a minimum between ~62° and ~67°, decreasing as λ increases, which corresponds to the condition of a symmetrical path of light inside the prism ($\beta = \beta'$). For λ = 532 nm, the minimum is for $\beta = \beta'$ = 63.8°.

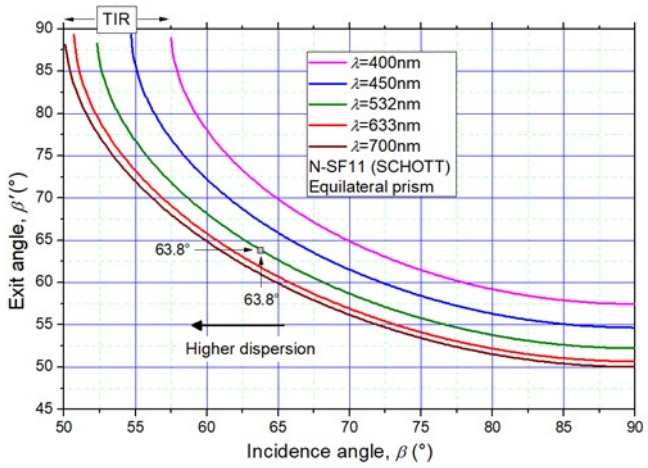

fig. 7. Exit angle *β′* of light from the prism, as a function of the angle of incidence at the entrance *β*, for five relevant Vis wavelengths.

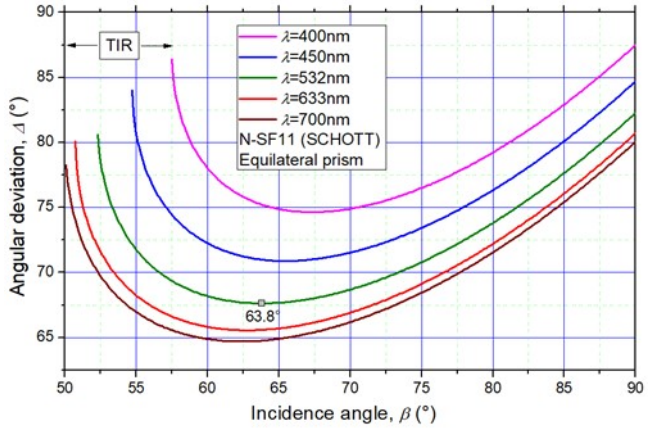

fig. 8. Angular deviation *Δ* of light from the prism, as a function of the angle of incidence at the entrance *β*, for five relevant Vis wavelengths.

This value of *β* is highlighted in the graphs as the experimental measurements in monochromatic light were carried out with a green (*λ* = 532 nm) He-Ne laser and in conditions close to a symmetrical light path. The angular deviation reaches the maximum values, above 80°, at the extreme values of the *β* interval. From Fig. 8, moreover, we can note the important aspect of the action of the prism, namely that all the curves present the maximum derivative, in absolute terms, at the lowest values allowed for the angle *β*, meaning that at these values there is the maximum angular dispersion of the wavelengths in the Vis. The same information is obtained from the trend of *β′*. We can conclude that the optimal angle to have the highest dispersion of light for the 400-700nm interval is the minimum one allowing the rays with *λ* = 400nm to exit the prism before undergoing the TIR. For *α* = 60° we have *χ* = 120°, and, as *n*(400nm) = 1.845 (see Eq. (13)), we have:

$$\sin\gamma' = 1/n = 0.542; \qquad \gamma' = 32.8° \qquad (14)$$

$$\gamma = \pi - \chi - \gamma' = 27.2° \qquad (15)$$

$$\sin\beta = \sin\gamma \cdot n = 0.842; \qquad \beta = 57.4° \qquad (16)$$

The angle β_{TIR} (*λ* = 400nm) = 57.4° is therefore the minimum angle that assures a strongly dispersed light in the range 400-700nm. To have the maximum angular dispersion of the Vis spectrum with the N-SF11 prism, therefore, we need to illuminate it at an input angle of around 60°.

III. Multiple Reflections in the Newton's Prism

Here we examine the behavior of the prism when multiple reflections are taken into account. Of course, we will only consider equilateral prisms, as only with them will it be possible to observe the optical effects we mentioned in the Introduction. Suppose we illuminate the equilateral prism N-SF11 with a ray of light, of unknown wavelength, λ_0, directed along the bisector of the angle formed by faces (1) and (3), and we imagine that this ray travels inside the prism parallel to face (3) (i.e. parallel to the edge of the base), as shown in Fig. 9. To know its wavelength, we apply Snell's law:

$$n(\lambda_0) = (\sin 60°) / (\sin 30°) = 1.73205 \qquad (17)$$

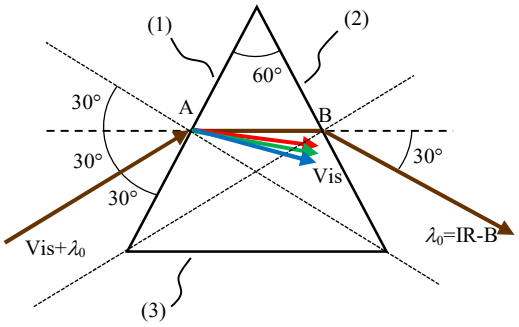

fig. 9. The prism is illuminated with a beam incident at 60° and containing the Vis spectrum and an unknown ray having a symmetrical optical path.

This ray corresponds to a wavelength of λ_0 = 2185.9 nm, i.e. to the infrared IR-B, beyond the visible region. This means that, if the incident bundle were white, distributed in the 400-700nm range, it would be subjected to a refraction angle slightly lower than 30° (between ~28° and ~29°), as qualitatively illustrated in Fig. 9, and therefore for no value of *λ* it would travel parallel to the base of the prism. If we want to have a path parallel to the side (3) by a particular wavelength of the Vis, such as 532 nm (green), the angle of incidence should be *β* = 63.8° (see Fig. 10). Then, analyzing the behavior in white light of the equilateral prism N-SF11, we will always consider an angle of incidence such as to have a path parallel to the side (3) for the particular wavelength λ_0 = 532nm.

Let us now return to the situation illustrated in Fig. 2, in which the light beam with *λ* = λ_0 is directed to the center of the side (1) of the prism and is refracted along the parallel to the side (3). In this case we know that the secondary ray, with the same wavelength λ_0, makes three reflections inside the prism before being refracted out of the side (2), overlapping with the primary refracted beam. Now let us imagine to slightly reduce the wavelength of the incident ray: *λ* = λ_0 – d*λ* (see blue ray in Fig. 11).

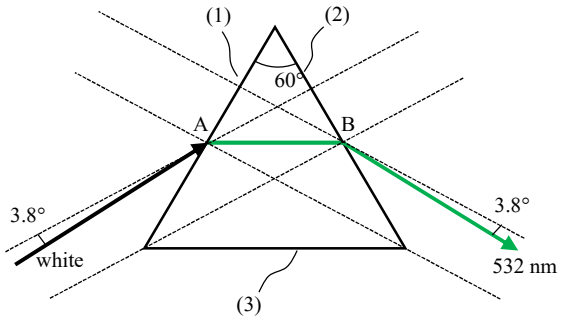

fig. 10. With an incidence angle of 63.8°, a green ray at λ = 532 nm runs along the N-SF11 prism parallel to side (3).

This ray will exit the prism as a primary ray with a refraction angle slightly higher than that with $\lambda = \lambda_0$: $\beta'(\lambda) = \beta'(\lambda_0) + d\beta'$. It is reflected in D, at a greater angle than that of λ_0, generating the secondary ray (dashed blue), striking point E at a smaller angle than that at λ_0; here it is reflected again and strikes point F at a greater angle than that at λ_0; here it is reflected again and strikes point G at a smaller angle than that at λ_0, and finally it is refracted and exits from point G at an angle lower than its primary with $\lambda = \lambda_0 - d\lambda$ and also with respect to λ_0. So, we find that the secondary ray with $\lambda = \lambda_0 - d\lambda$ undergoes, leaving the prism, an angular deviation CCW with respect to its primary, thus moving beyond the direction of the primary with $\lambda = \lambda_0$. This happens for all wavelengths less than λ_0.

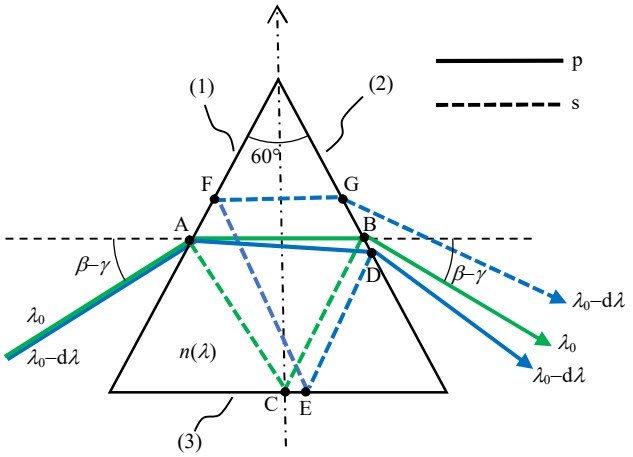

fig. 11. The prism is illuminated by two light beams with λ_0 (green) and $\lambda_0 - d\lambda$ (blue) wavelengths. The green beam follows a symmetrical path inside the prism.

If we now consider incoming rays with wavelengths slightly higher than λ_0, we will have a reversed situation, that is all the secondary rays with $\lambda = \lambda_0 + d\lambda$ will undergo, at the prism output, an angular deviation CW with respect to the own primary, thus moving beyond the direction of the primary with $\lambda = \lambda_0$.

We begin to analyze, for simplicity, the exit angle of only two rays of the visible spectrum, one green and one red, which travel parallel and affect the prism in the same point. After the refraction on the side (1), they will diverge by the angle $\Delta\gamma$ and the red ray will strike the side (2) with a smaller angle than the green ray (see Figs. 12a and 12b). This divergence will be kept following each internal reflection in the prism, but, after each reflection, they will exchange roles (see Figs. 12b, c, d). The final result is that, after an odd number of reflections, they will strike again the side (2) in opposite way with respect to the two primary rays, that is the red ray will strike the side (2) with a greater angle than the green ray (see the sequence of figures from Fig. 12a to Fig. 12e).

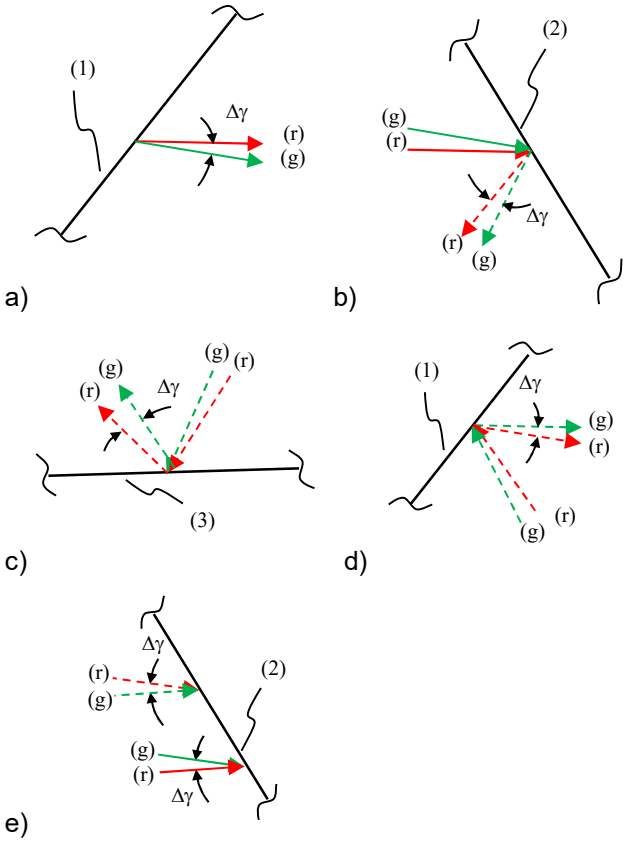

fig. 12. The sequence of the interactions of the green and red rays, primary and secondary, with the internal walls of the prism is shown.

We are now able to calculate the refraction angle of the primary and secondary rays, taking into account the variation of the angles of incidence of the secondary rays within the prism. Let us consider a ray internal to the prism and incident on the wall (2) with angle γ_1 (see Fig. 13). The ray meets the wall (3) at an angle γ_2. Knowing that the angle χ between any two normal to the faces of the equilateral prism is: $\chi = \pi - \alpha = \pi - \pi/3 = 2/3\ \pi$, the angle γ_2 will be:

$$\gamma_2 = \pi - \gamma_1 - 2/3\ \pi = \pi/3 - \gamma_1 \quad (18)$$

The same relation is applied when the ray strikes the wall (1) with angle γ_2 and again the wall (2) with angle γ_4, for which we will have:

$$\gamma_4 = \pi/3 - \gamma_3 = \pi/3 - (\pi/3 - \gamma_2) = \pi/3 - \gamma_1 \quad (19)$$

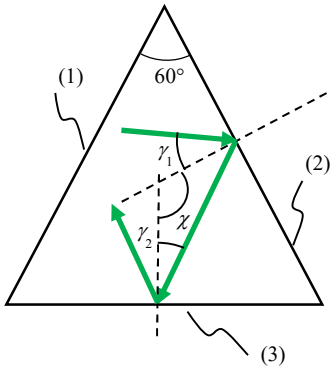

fig. 13. Two successive reflections within the prism and the respective angles.

As it can be seen from Eq. (19), when $\gamma_1 = \pi/6$, then also $\gamma_4 = \pi/6$, that is, only when $\gamma_1 = 30°$ the reflected ray returns on the wall (2) with the same angle; in all other cases, the angle of incidence changes in the passage from primary to secondary ray. Thus, in a prism with $\alpha = 60°$, at each reflection, an internal ray previously incident with angle γ, in the subsequent reflection will be incident at an angle $(\pi/3 - \gamma)$, which means that the rays that make an even number of reflections before returning to the same wall do not change their angle of incidence, while those that make an odd number of reflections change their angle of incidence from γ to $(\pi/3 - \gamma)$.

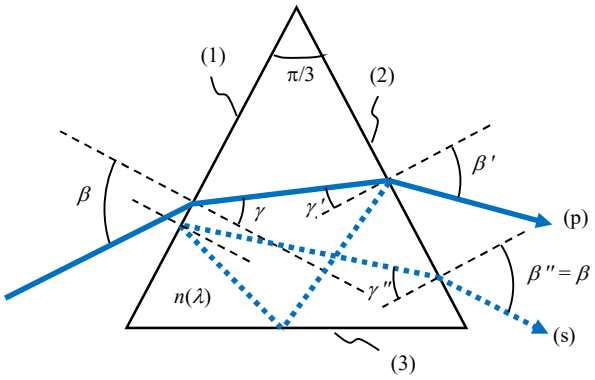

fig. 14. The output angles β' and β'' of a beam for a generic input angle β are highlighted.

Let us now calculate the exit angle β'' of a secondary beam, referring to Fig. 14. We have:

$$\sin\beta'' = n\sin\gamma'' = n\sin(\pi/3 - \gamma') = n\sin[\pi/3 - (\pi/3 - \gamma)] = \ldots$$
$$\ldots = n\sin\gamma = n(\sin\beta / n) = \sin\beta; \quad \beta'' = \beta \qquad (20)$$

Eq. (20) tells us that the secondary ray has an exit angle from the prism equal to the entrance angle, regardless of the impact point on the prism of the incoming ray and of the wavelength. Therefore: "If we have a beam of white light at the entrance, we will have at output a dispersed primary beam and a non-dispersed secondary beam, that is still white". Qualitatively the situation can be illustrated as in Fig. 15. As can it be seen from Fig. 15a, the two output beams will generally have a different divergence: $\beta'' \neq \beta'$ (where β' is referred to the green ray). The secondary white beam, instead, always keeps an exit angle equal to the input of the primary beam: $\beta'' = \beta$; in this case the two output beams can be observed separately on a far screen. If the white incoming beam, however, is regulated in such a way that its central λ_0 (for example the green) travels parallel to the side (3) inside the prism, or that we have: $\beta'_{green} = \beta$, then it will also be $\beta'' = \beta'_{green}$ and the two beams will travel parallel at output (see Fig. 15b). In this case, if the incoming beam strikes the central point of the prism side (1), the two output beams will also be overlapping and, given the higher intensity of the dispersed beam, the secondary one will not be visible. If instead the incoming beam strikes a point distant from the centre of the side (2), as has already been suggested with Fig. 3, then the two output beams will still be parallel, but not overlapping (see Fig. 15c) and therefore they can be observed separately.

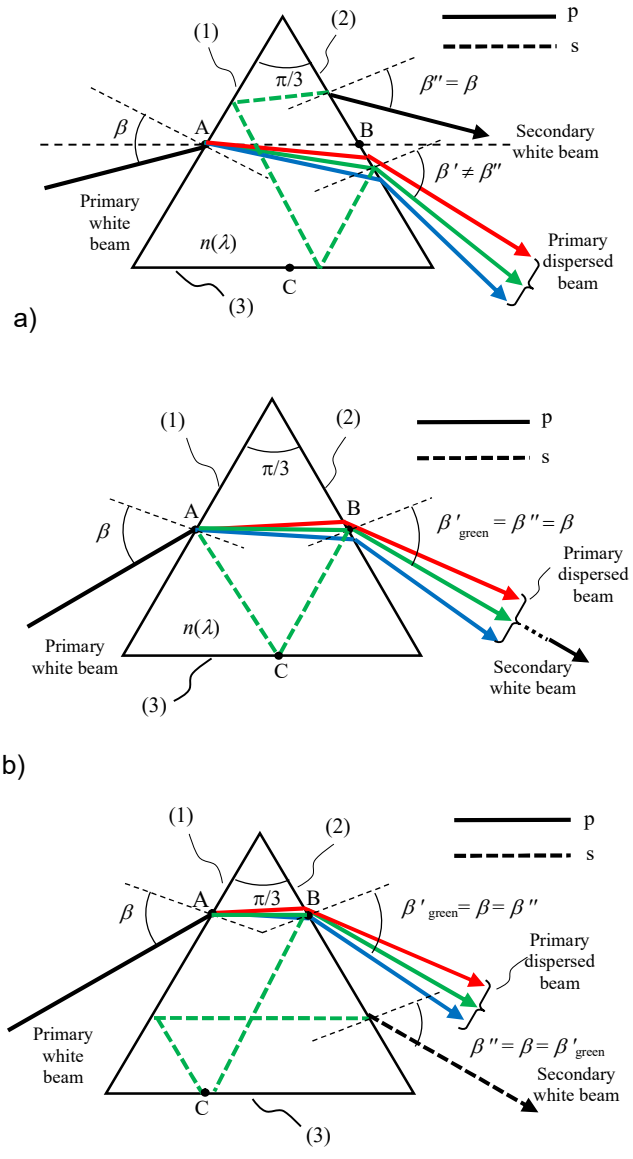

fig. 15. The configuration of primary and secondary refracted rays is shown in various conditions of incidence of the incoming white beam; (p) = primary, (s) = secondary.

If we continue to follow the internal reflections of the secondary rays, we would find that, after a second round CW inside the prism, that is after a total of six internal reflections, according to what defined by Eq. (18), the secondary rays would affect the face (2) with the same angles that gave rise to the dispersion of the primary beam, and therefore we expect to have an additional secondary dispersed beam after six (even number) internal reflections. In principle, this process never ends, provided we go on to consider ever lower light intensities, at the infinitesimal limit. From the experimental point of view, we expect to see, leaving the face (2), only the dispersed primary beam and the first white secondary beam. As we will see in Section VB, using a fairly intense green laser beam (~100mW), it is possible to observe the secondary beam. As expected, by moving the point of incidence of the laser on the prism, or slightly rotating the prism, the two beams, primary and secondary, can be well distinguishable. In Table 1 we summarize the main properties expected for the beam exiting the face (2) of the prism, illuminated on the face (1) by a parallel beam of white light.

TABLE I. TYPE OF RAYS EXITING FACE (2) OF THE PRISM, ILLUMINATED ON FACE (1) BY A PARALLEL WHITE BEAM. ALL SECONDARY RAYS ARE PRODUCED BY A NUMBER OF REFLECTIONS MULTIPLE OF 3.

Number of internal reflections	Order	Beam property	Origin
0	Primary	Dispersed	Refraction
3	Secondary	White	″
6	″	Dispersed	″
9	″	White	″
…	″	…	″

It is interesting to examine the behavior of the prism when it is completely illuminated on two sides (e.g. (1) and (3)) by a parallel white light directed along one of its bisectors, that is with $\beta = 60°$ (see Fig. 16), as this condition will be examined in the experimental Section VB. Now the face (1) is completely illuminated, therefore from all the points of the face (2) come out the rays that correspond both to the dispersed primary beam, and to all the secondary beams, in particular to the more intense white one after three internal reflections, that comes out of the prism with the same angle as the input beam, i.e. 60°. The primary dispersed beam, imagined centered on the green (λ_0 = 532nm), no longer travels parallel to the sides of the prism and comes out with an angle β'_{green} given by:

$$\beta'_{green} = \sin^{-1}\{n \cdot \sin[\pi - \chi - \sin^{-1}(\sin(\pi/3)/n(\lambda_0))]\} = 68.2° \quad (21)$$

and then it is inclined by 8.2° CW with respect to the white secondary beam. In the same direction of these beams, i.e. to the right of the prism and downwards (see Fig. 16), we now also find all the rays that are due to the primary beam incident on the face (3). This primary produces a very intense white beam due to reflection on face (3), as well as all the secondary rays due to the following number of reflections inside the prism (see Table 2): 2, 2 + 3 = 5, 5 + 3 = 8, 8 + 3 = 11…, which give rise to a dispersed secondary beam, then to a less intense white beam, then to an even less intense dispersed beam, and so on. That is, the secondary beams produced by the beam incident on face (3), and coming out of the same face, are also a succession of alternated white and dispersed beams due to the alternation of the parity of the number of internal reflections to which they are subjected. Table 2 summarizes the main properties of the beam exiting the face (3) of the prism, due to the illumination of the same face with parallel white light.

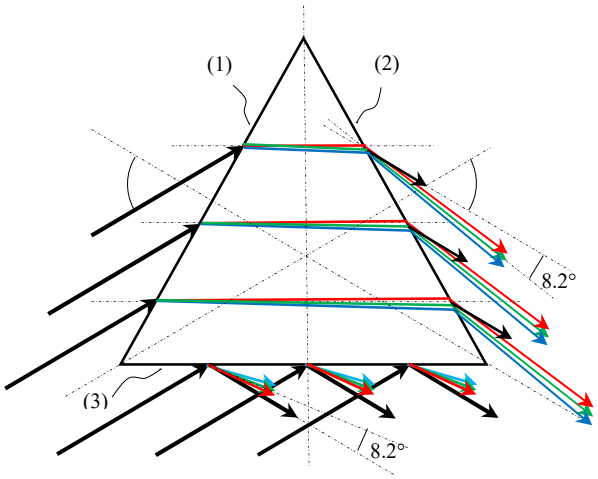

fig. 16. The prism is illuminated on the faces (1) and (3) with a parallel beam of white light directed along the bisector.

TABLE II. TYPE OF RAYS EXITING FACE (3) OF THE PRISM, ILLUMINATED ON THE SAME FACE BY A PARALLEL WHITE BEAM. WE CALL "SECONDARY" ALL THOSE RAYS THAT ARISE AFTER HAVING UNDERGONE REFLECTIONS INSIDE THE PRISM.

Number of internal reflections	Order	Beam property	Origin
0	Primary	White	Reflection
2	Secondary	Dispersed	Refraction
5	″	White	″
8	″	Dispersed	″
…	″	…	″

In Fig. 16 it is shown that the dispersed secondary beam leaving the face (3) is not aligned with the reflected white beam, but is rotated by 8.2° CCW, i.e. its exit angle is β' = 68.2°, as in case of the dispersed primary beam leaving the face (2). In fact, it is produced by two (an even number) internal reflections that do not change the angle of incidence on the inner face of the prism, as can be seen by applying twice the Eq. (18). This dispersed beam would be much less intense than that coming out of the face (2), because it would have undergone two internal reflections; nevertheless, as we shall see, it can still be observed.

The interesting thing to note in Fig. 16 is that the two dispersed beams coming out of the faces (2) and (3) have the colors reversed, as it happens in the rainbow with the first and second orders. From an experimental point of view, realizing the condition illustrated in Fig. 16, and placing a white screen far from the prism on the lower right side, it should be possible to distinctly observe the two dispersed beams, with the colors reversed, because they diverge by 16.4°, and at the center of them should be observed the very intense white beam due to the reflection on the face (3). To observe the white secondary coming out of the face (2), superimposed on that intense reflection, it would be necessary to obscure the face (3). The origin face of the beams projected on the screen would in fact be easily identifiable by alternately obscuring the faces (1) and (3). A better representation of what happens by illuminating the prism with white light, can be done by imagining to illuminate only one face of the prism, instead of two, but examining all the luminous components coming out of the three faces, as illustrated in Fig. 17. The various components are obviously of increasingly lower intensity as the number of internal reflections increases, which I have qualitatively represented by reducing the length of the arrows. The black arrows represent the white beams, while those in three colors represent the dispersed beams. The beams are numbered starting from <0> for the incident beam, which is directed along the axis – ξ, corresponding to a bisector of the prism; <R> is the reflected white beam, <1> is the primary dispersed beam, <2> is the secondary white beam, <3> is the dispersed secondary beam, and so on. For practical reasons, they are indicated up to the number <8>, secondary white. In Fig. 17 we have represented only the incident beam at the center of the face (1), but if the whole face was illuminated, the optics of the prism would be the same, that is we will have the secondary beams directed towards similar directions and having the same optical properties. The white secondary beams are directed along three different directions, at 120° from each other, corresponding to the directions of the three bisectors of the prism.

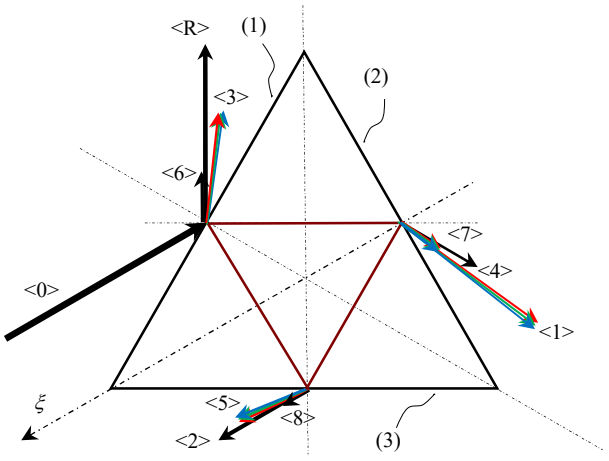

fig. 17. The most intense beams coming out of the prism, illuminated only on the face (1), are shown.

The dispersed secondary beams are instead rotated slightly clockwise with respect to the white ones (for the precision of 8.2°, as shown in Fig. 16, having decided to consider the wavelength of 532 nm as the central one of the dispersed rays), but still maintain a 120° difference among them. Now, if we illuminate only the face (3) of the prism with the same parallel white beam directed along the same direction – ξ, we will have a result identical to that found by illuminating the face (1), but symmetrical with respect to the axis ξ. By illuminating both faces (1) and (3) of the prism, we will have the sum of the secondary beams found illuminating the two faces separately. In the latter case, by placing a white screen far below on the right, we could observe (referring only to the primaries and secondary shown in Fig. 17) the following beams: <R>, <1>, <3>, <4 >, <6> and <7>. In practice, we expect to see only the bundles <R>, <1>, <3> and <4>, which are the most intense. By illuminating two faces of the prism, (1) and (3), with a parallel white beam as shown in Fig. 18, we will ultimately have three groups of beams coming out of the three faces of the prism and directed along the three bisectors of the prism, ξ, ψ and ζ. The beams of type <R>, <3>, <6>, ... and <1>, <4>, <7>, ... will be directed towards directions ψ and ζ, while the beams of type <2>, < 5>, <8>, ... will be directed towards the ξ direction, that is against the incident beam <0>.

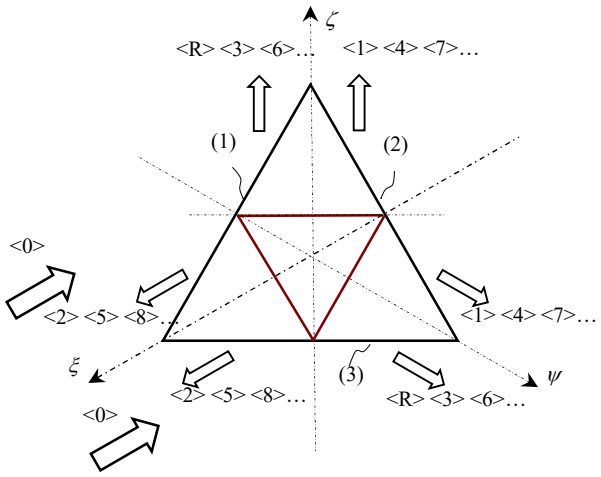

fig. 18. The prism is illuminated by white beams parallel to the ξ axis on the two faces (1) and (3).

If we identify the various beams with the symbols: "p" = primary; "s" = secondary; "r" = reflected; "d" = dispersed; "w" = white, then the series of beams issued by the prism become: <R> = p, r; <1> = p, d; <2> = s, w; <3> = s, d; <4> = s, w; <5> = s, d; <6> = s, w; <7> = s, d; <8> = s, w…. The beams refracted by the individual faces of the prism, when it is illuminated on the face (1), form a sequence of the type: <3n + 1> exiting the face (2), <3n + 2> exiting the face (3) and <3n + 3> exiting the face (1), with n natural number (0, 1, 2, ...).

IV. Further Discussions on the Reflections Within the Prism.

A. Reverse Prism (RP): White Light Inside

In one of his best-known experiments, Isaac Newton dispersed a beam of sunlight into its colour spectrum by using a prism. Then he sent the dispersed

light to a second prism, oriented so as to bend the light beam oppositely with respect to the first prism. The various coloured rays were in this way recombined to get white light again [20, 24-28]. Here, we examine a new method to manipulate the light with an equilateral prism, following which this is lighted with a dispersed light beam in such a way that all the wavelengths are refracted internally at the same angle (30°), forming a white light beam, as shown in Fig. 19a.

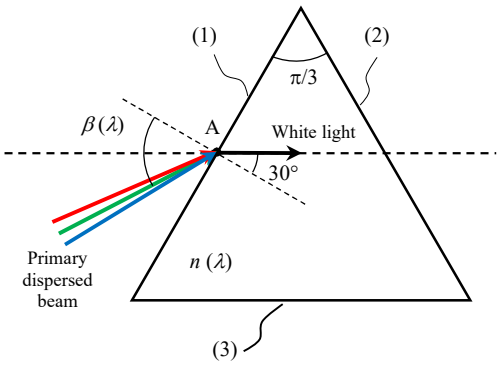

a)

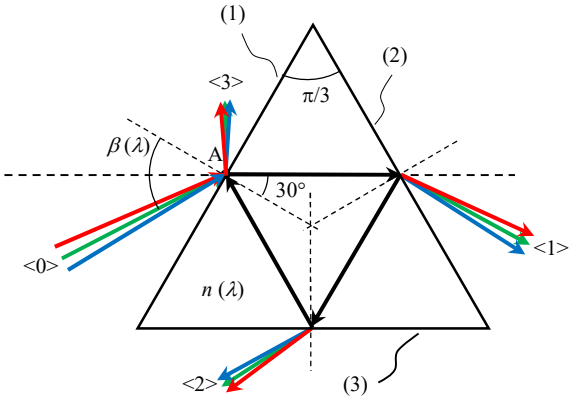

b)

fig. 19. (a) Equilateral prism illuminated with a dispersed beam incident at angle β(λ) in such a way as to have a refraction angle independent of λ and equal to 30°. (b) The incident dispersed primary beam and three refracted dispersed secondary beams are shown. The reflected dispersed beam is not represented.

If at the first refraction the beam is white, then it must remain so after every internal reflection, whatever the number of reflections made, because the reflection does not produce spectral dispersion. What happens, therefore, is that, on every wall of the prism, in correspondence of every reflection, the light will be refracted outside reproducing the dispersion that it had at the entrance. In Fig. 19b only the refracted and dispersed beams <1>, <2> and <3> are shown, coming out clockwise from the single faces of the prism, excluding the dispersed beam reflected from the face (1) and taking into account only qualitatively of the intensity, which, obviously, will decrease noticeably after each reflection / refraction at the glass / air interface. In Fig. 19 we impose an internal refraction angle γ_0 = 30°, common for all wavelengths. The entrance angle will be $\beta = \beta(\lambda)$, and must respect the Snell's law:

$$\sin\beta(\lambda) = \sin\gamma_0 \cdot n(\lambda) = n(\lambda)/2 \qquad (22)$$

The refractive index is known (see Eq. (13)), so it is possible, in principle, to adjust the spectral incidence angle $\beta(\lambda)$ so as to respect Eq. (22). Fig. 19 shows a dispersed light beam striking face (1) near the center. Of course, nothing changes if the light illuminates the whole face (1) of the prism, and the rays, at the same λ, will keep the same directions at the exit from the prism. Of course, all the beams reflected or refracted outside the prism will be dispersed, while the inside of the prism will be crossed only by white light. In the previous discussion, instead, the prism was always crossed by dispersed light, in the sense that the various rays at different λ maintained the same angular mutual divergence, even after every reflection on the faces of the prism, that behaved like mirrors, while at the outside the light could be white or dispersed. What changed, after each reflection, was only the angle of incidence on the faces of the prism, which ultimately resulted in a white or dispersed beam.

B. A Practical Realization of the Reverse Prism (RP)

A simple experiment that could be done with the Reverse Prism, before experimenting with white light, is to illuminate the prism with two laser beams, for example one green (532nm) and one red (633nm), orienting them on the prism to the angle obtained by applying Eq. (22). The two beams will be combined inside the prism forming a yellow beam and will come out of the prism, dispersed, with the same entry angles. It is possible to realize in practice what is illustrated in Fig. 19, that is to realize a Reverse Prism, combining the equilateral, triangular, prism with a trapezoidal prism as shown in Fig. 20. This prism will have the face (2) inclined of 30° with respect to face (1), in such a way to be parallel to face (1) of the equilateral prism. If illuminated on the face (1) as shown in Fig. 20, the white light beam will cross the trapezoidal prism without being dispersed and will strike the face (2) at an angle of 30°. The dispersed beam refracted externally will illuminate the face (2) of the equilateral prism by striking at the same spectral angle $\beta(\lambda)$ with which it came out of the trapezoidal prism; consequently, the internally refracted beam will be white. Of course, for this experiment to work, the trapezoidal prism must have the same refractive index of the triangular prism. To optimize this experiment, it is useful to prepare an anti-reflective coating (ARC) on the faces (1) and (2) of the trapezoidal prism and on the three faces of the equilateral prism.

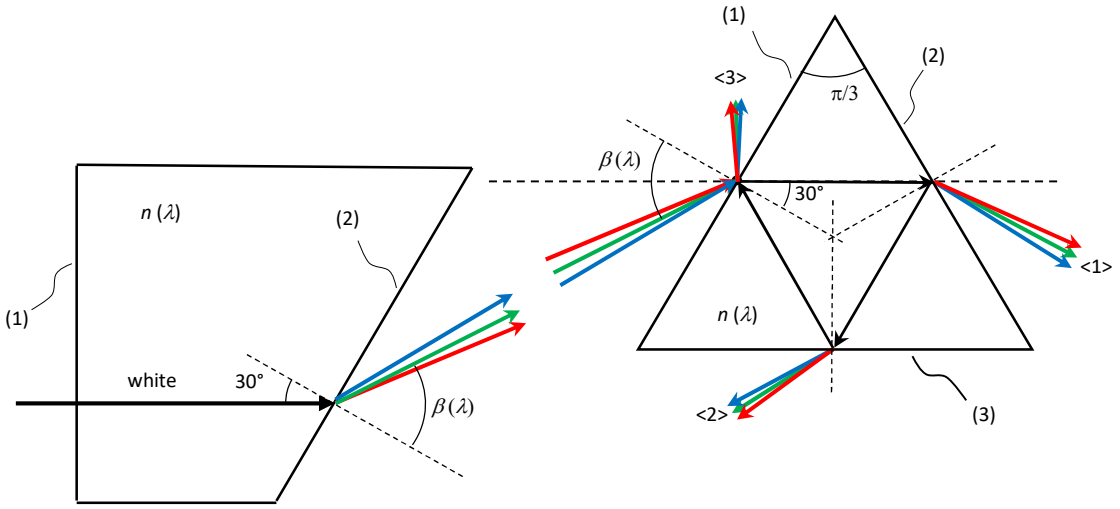

fig. 20. Schematic diagram showing the possible application of the Reverse Prism (RP) method, using a trapezoidal prism suitably coupled with the equilateral triangular prism.

TABLE III. TYPE OF RAYS EXITING FACE (3) OF THE PRISM, ILLUMINATED ON THE SAME FACE BY A PARALLEL WHITE BEAM. WE CALL "SECONDARY" ALL THOSE RAYS THAT ARISE AFTER HAVING UNDERGONE REFLECTIONS INSIDE THE PRISM.

Beam	**Measured Polarization**	***I* (lx)**	***I*$_{sper}$ (%)**	***I*$_{theo}$ (%)**		**Measured Polarization**	***I* (lx)**	***I*$_{sper}$ (%)**	***I*$_{theo}$ (%)**
<0>	*p*	1218±5	100±0.4	100		*s*	1265±5	100±0.4	100
<R>	*s*	6±5	0.5±0.4	0.2		*s*	370±5	29.2±0.5	31.1
<1>	*p*	1210±5	99.3±0.8	99.6		*s*	602±5	47.6±0.6	47.5
<2>	*p*	3±5	0.2±0.4	0.2		*s*	172±5	13.6±0.4	14.8
<3>	*s*	≈0	≈0	≈0		*s*	50±5	4.0±0.4	4.59
<4>	*s*	≈0	≈0	≈0		*s*	15±5	1.2±0.4	1.43
<5>	*s*	≈0	≈0	≈0		*s*	6±5	0.5±0.4	0.445
<R>+<3>	*s*	5±5	0.4±0.4	0.2	(†)	*s*	424±5	33±0.5	35.7
<1>+<4>	*p*	1200±5	98±0.8	99.6	(†)	*s*	594±5	47±0.6	48.9
<2>+<5>	*p*	3±5	0.2±0.4	≈0	(†)	*s*	161±5	12.7±0.4	15.2

V. IRRADIATION WITH MONOCHROMATIC LIGHT.

A. Theoretical Aspects

Let us now proceed with the calculation of the intensity of the various beams coming out of the prism, when this is illuminated by monochromatic parallel light at 532 nm (green), polarized "*p*" or "*s*", which crosses the prism with a symmetrical path, that is, keeping itself always parallel to its faces. The angle of entry of the light will then be: $\beta = 63.8°$ (see Figs. 7 and 8). The intensity values found will then be compared with those measured experimentally. The procedure followed for calculating the intensities of the reflected or refracted beams with monochromatic light is shown in Appendix A. It is based on the use of the Fresnel equations [29], which give the reflectivity $\mathcal{R}$ and the transmissivity $\mathcal{T}$ of the light through the air/glass or the glass/air interface (the equations are symmetrical with respect to the angles of incidence and refraction), in correspondence with the two polarizations "*p*" and "s": $\mathcal{R}_P$, $\mathcal{R}_S$, $\mathcal{T}_P$, $\mathcal{T}_S$. Then, given the intensity of the incident beam $I_0 = 1$, the intensity of the reflected beams will be:

$$I_R^p = \mathcal{R}_P; \qquad I_R^S = \mathcal{R}_S \tag{23}$$

While the intensity of the refracted beams will be:

$$I_n^p = \mathcal{R}_P^{n-1} \cdot \mathcal{T}_P^2; \qquad I_n^s = = \mathcal{R}_S^{n-1} \cdot \mathcal{T}_S^2 \tag{24}$$

Eq. (24) must be interpreted in this way: the intensity of the refracted beam of order <n> (n = 1, 2, 3, ...) is the result of two transmissions, one towards the inside and one towards the outside of the prism, which involve an attenuation equal to $\mathcal{T}^2$, and of a number (n–1) of internal reflections, each with attenuation $\mathcal{R}$, which involve an attenuation of $\mathcal{R}^{n-1}$. The theoretical values I_{theo} of intensity of the various beams, for $\lambda = 532$ nm and a symmetrical path, are shown in Tab. III. For each incident beam leaving the prism is reported: i) the measured polarization state, ii)

the measured intensity in lux and iii) the intensity in (%) with respect to the incident beam, both theoretical and experimental. From it we observe that, with "*p*" polarization, $\mathcal{R}_P$ is very small, as well as all the beams <n> with n ≥ 2, and therefore we have in practice the dominant beam <1> in output, the rest is negligible. In polarization "*s*", on the other hand, $\mathcal{R}_S$ is of the order of 0.3, and the intensity of the incident beam is distributed on the various refracted beams, albeit with gradually lower intensities, making it possible to experimentally measure several refracted beams, until <5>. Actually, a sixth refracted beam was observed, very little intense. Table 3 also shows the experimental intensity values, which have been measured as described in the following section VB. The note (†) in Table 3 indicates that, due to experimental errors, the intensity of the sum of two beams does not always correspond to the sum of the individual intensities. The beams with anomalous polarization and very low intensity were set to zero.

B. Experimental Measurements

Fig. 21 shows the diagram of the experimental apparatus used for measurements with monochromatic light. The experimental measurements were carried out with green laser light (λ = 532 nm). A commercial solid-state laser (LA), with 100 mW power, was connected to an external DC power supply (PS), regulated to have a stable output power: V_{DC} = 2.7 V, I_{DC} = 0.3 A. A cooling fan (FA) was used to cool the laser and stabilize its temperature. A fraction (~10%) of the incident light was reflected by the beam splitter (BS) to be monitored, and was measured with the system comprising the integrating sphere (IS1), the sensor (SE1) and the luxmeter (LX1) (Lutron LM-8000). The beam transmitted by (BS) was then polarized by the polarizer (PO1), adjusted so as to transmit to the prism (PR) a polarized beam "*p*" or "*s*". The measurement of the intensity of a beam exiting the prism was made by intercepting it with the integrating sphere (IS2), connected, via the sensor (SE2), to the luxmeter (LX2) (Lutron LX-1102). The two integrating spheres were manufactured in the laboratory starting from plastic garden globes, first practicing the holes for the entry and exit of light, then blasting the internal and external surfaces and painting them with a white paint, then painting the external surface with a black paint, and finally painting the internal surface with a dozen steps of a solution of $BaSO_4$ + white vinyl glue [30, 31].

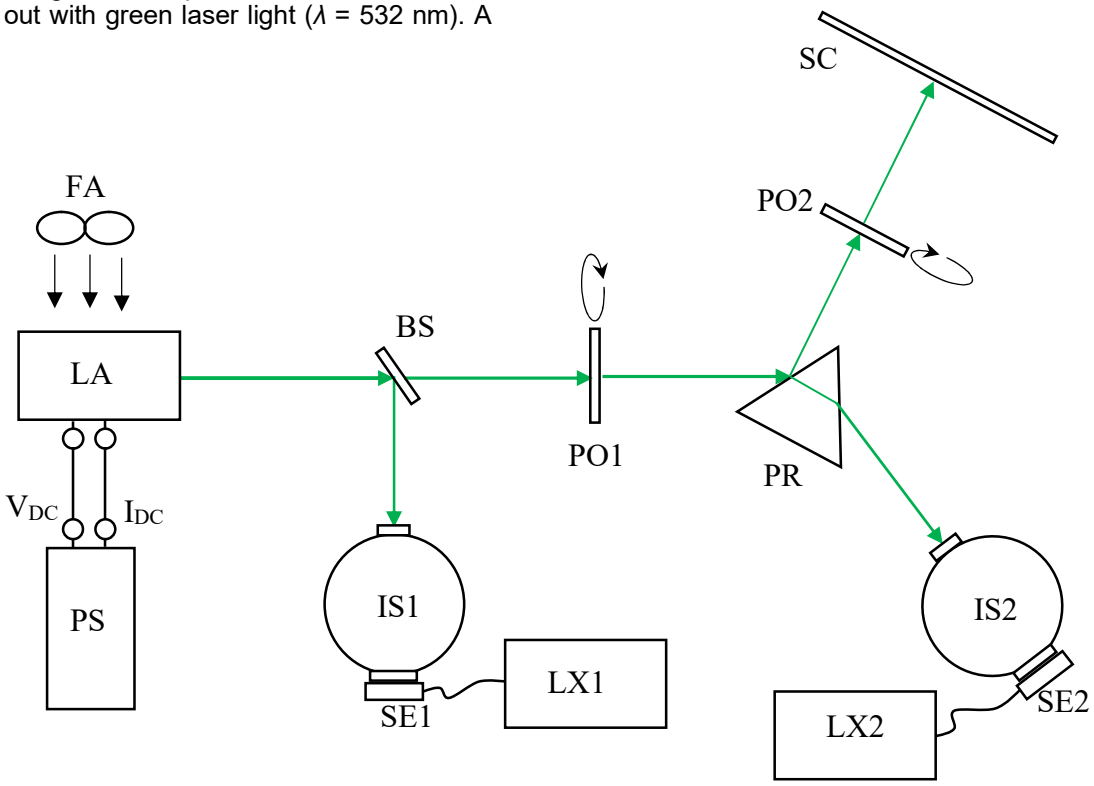

fig. 21. Diagram of the experimental apparatus for measuring the state of polarization and the intensity of the laser beams. Legend: PS = Power Supply; LA = Laser; FA = Fan; BS = Beam Splitter; IS = Integrating Sphere; SE = Sensor; PO = Polarizer; LX = Luxmeter; PR = Prism; SC = Screen

Since light is monochromatic, the lux measurements are proportional to the radiometric ones, which is sufficient to have the intensity of the output beams relative to that of the inlet beam. To measure the polarization state of a beam exiting from the prism, the polarizer (PO2) was used together with the white screen (SC) and the intensity of the spot on the screen was observed during the polarizer rotation; alternatively, the polarizer (PO2) was interposed between the prism and the integrating sphere (IS2) to make a quantitative measurement of intensity. In principle, when working in "*p*" polarization, all the output beams should be of the "*p*" type, and vice versa in the case of the "*s*" polarization, because the two types of waves are independent of each other. In practice, due to the fact that the electric field of the

incident laser beam, linearly polarized, is not perfectly aligned with the incidence plane in polarization "*p*", or orthogonal to it in polarization "*s*", it follows that the prism receives a small unwanted component which is then transmitted to the output beam. Therefore, with low intensity beams, it can happen to measure at output a polarization "*s*" also working in polarization "*p*", and vice versa. This is what is observed in Tab. III.

As we have already seen, when the input angle β = 63.8°, the refraction angle γ = 30° for λ = 532nm. This condition means that also β' = 63.8° and that the rays are reflected internally at the same angle of 30°. For reasons of symmetry, all the rays, both those reflected from the face (1) and all those refracted, will be transmitted by the prism to the same angle of exit of 63.8°. Experimental measurements were made by setting an input angle close to 63.8°. However, to distinguish well and measure the intensity of beams forming pairs of overlapping rays, this angle has been slightly changed. Intensity measurements have been made, however, also on pairs of superimposed rays (see notes (†) in Table III).

The experimental intensity, in lux, of the various beams is shown in Tab. III for the "*p*" and "*s*" polarization states of the incident beam. The intensity values, translated into (%) with respect to the intensity of the incident beam, were then compared with the theoretical ones. The intensity values of a few units, especially those relating to an anomalous polarization, have been set equal to zero.

The anomalous polarization occurs when a polarization different from the set one is measured and the cause is a non-optimal alignment between the polarizer and the prism. Tab. III shows that, in polarization "*p*", as it was theoretically found, the only measurable beams at the exit of the prism are the reflected one <R>, not very intense, and the refracted one <1>, very intense; all the other beams are negligible. In polarization "*s*", on the other hand, all the beams outgoing from the prism were polarized "*s*", as expected, and their intensity has been measured for beams from <1> to <5>. The agreement between the theoretical and experimental values of the intensity of the various beams is satisfactory, taking into account the experimental errors.

Some photos of the experimental apparatus are shown in Fig. 22. Fig. 22a shows the optical bench with all the components used during the projection of the laser beams on the screens: the pairs of beams <R> + <3> on the right screen and the pairs of beams <1> + <4> on the left screen, in polarization "*s*". Fig. 22b shows the experimental apparatus during the measurement of the intensity of the beams <1> and/or <4>, using the integrating sphere (IS2) and the sensor (SE2). Finally, Fig. 22c shows the experimental apparatus during the measurement of intensity of the incident polarized beam <0>, through the integrating sphere (IS1) and the sensor (SE1).

a)

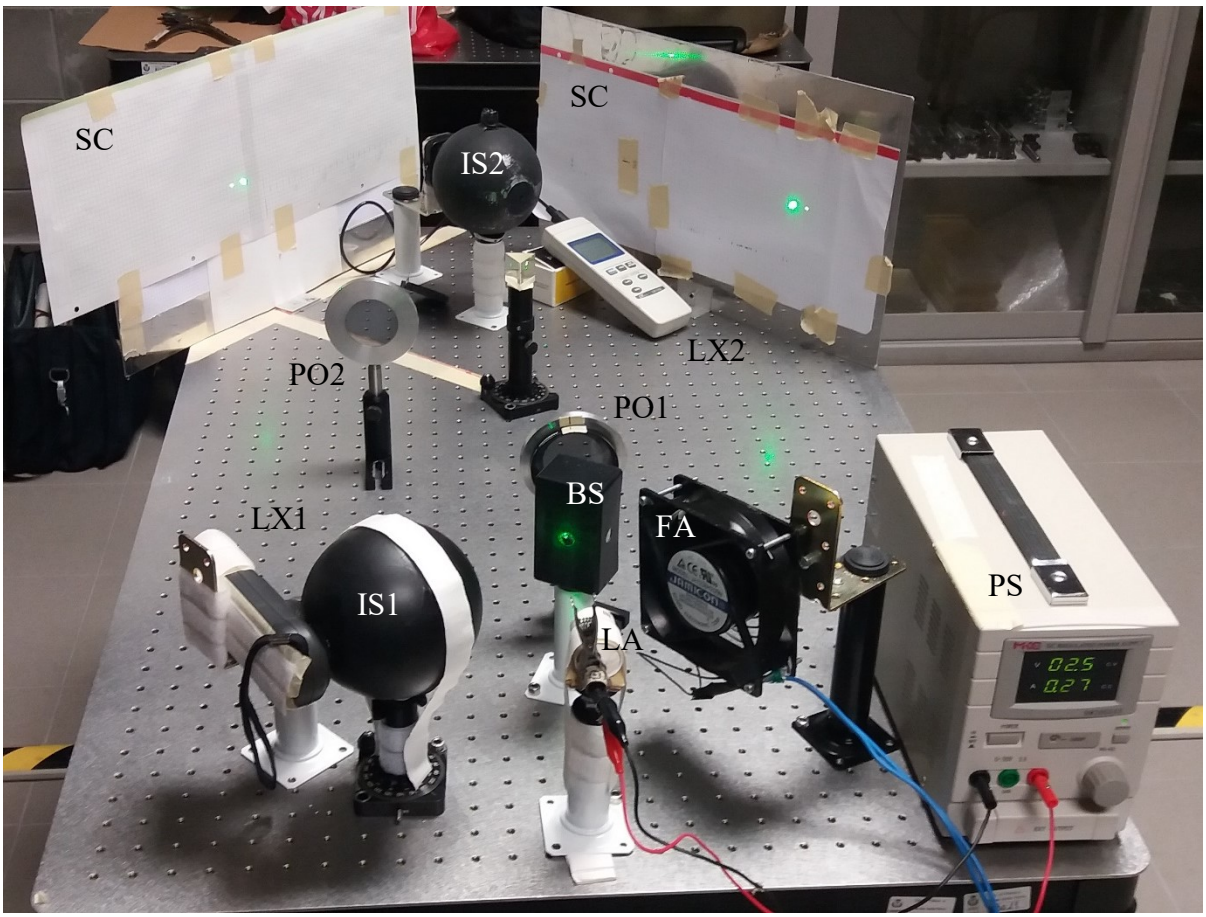

b)

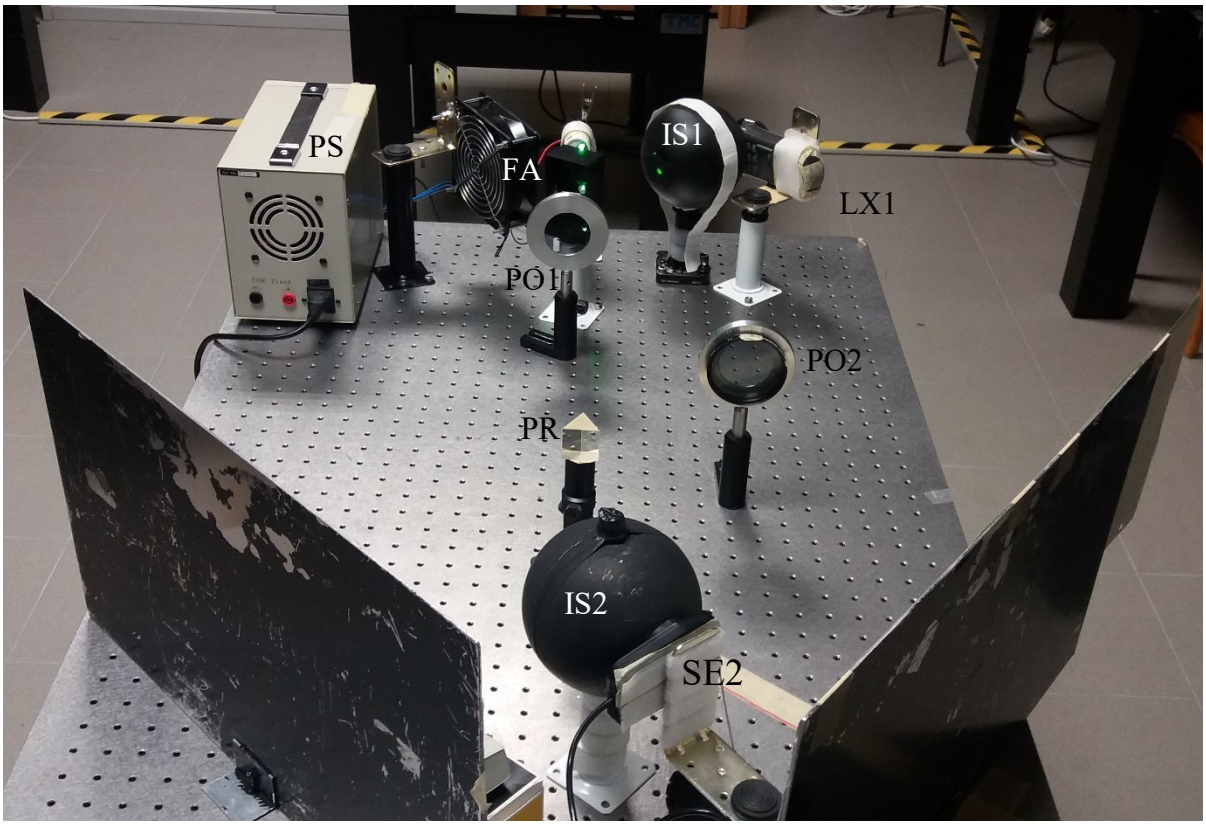

c)

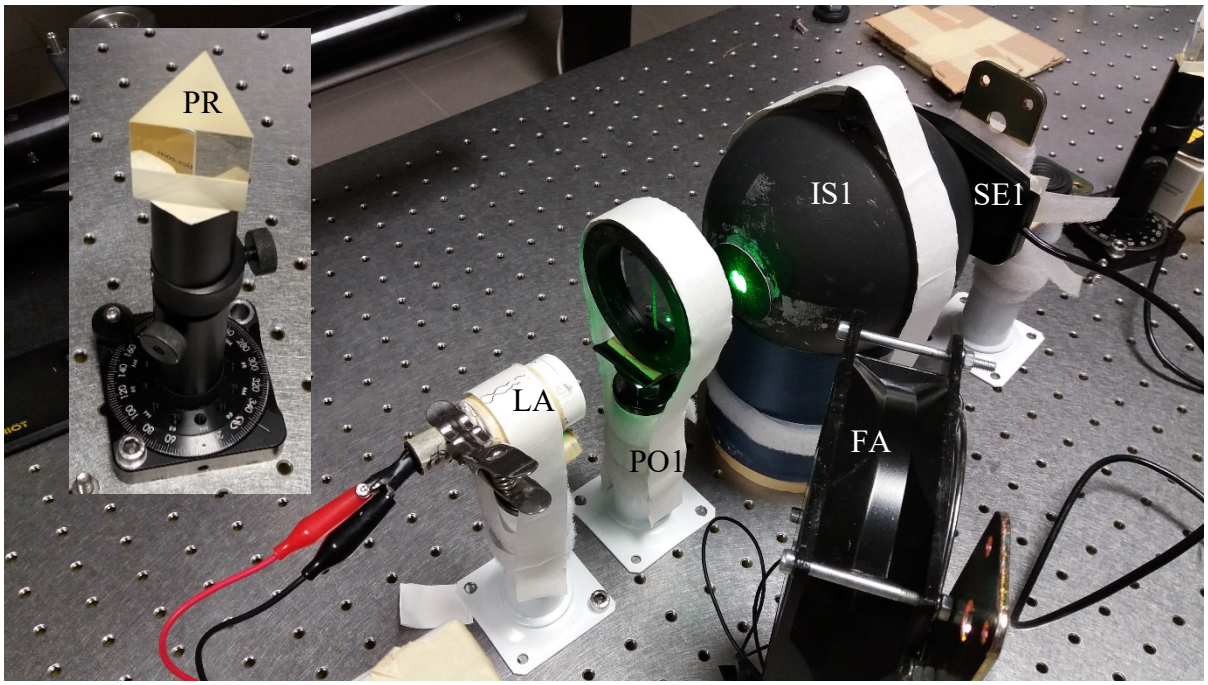

fig. 22. Some photos of the experimental apparatus are shown. a) Overall view of the apparatus from the side of the laser source. b) Overall view of the apparatus from the prism side. c) Detail of the intensity measurement of the polarized laser beam and an enlarged view of the SCHOTT prism N-SF11 in the insert.

VI. IRRADIATION WITH WHITE LIGHT.

A. Theoretical Aspects

We now look for the spectrum of light coming out from the prism when it is illuminated by a white light. More precisely, assuming a flat spectrum, $I_0(\lambda) = 1$, for the light in the range 400-700nm at the entrance of the prism, we want to find how this spectrum is modified in the various beams coming out of the prism. We will consider input light polarized "*p*" or "*s*" and unpolarized light, maintaining the previous conditions with regard to the angle of incidence of the incoming beam, that is equal to 63.82°, which involves an internal refraction angle equal to 30° for the green light at 532nm, which will therefore continue to cross the prism internally, always remaining parallel to the individual faces. The

procedure adopted for the detailed calculation of the spectral intensities of the beams coming out of the prism is reported in Appendix B. In the following, as already done with monochromatic light, we will talk about spectral reflectivity or spectral transmissivity instead of spectral intensity, because, for simplicity, we imagine an incoming spectral intensity constant and unitary.

We now apply the equations reported in Appendix B to the polarization of type "*p*". The reflected beam shows a very low relative intensity, with an attenuation maximum at 400 nm which reduces at increasing wavelength (see Fig. 23a). That the <R> beam is very low is explained by the fact that we are working with an entrance angle of 63.82°, close to the Brewster angle (see Eq. 16 for n (λ = 532nm)):

$$\beta_{brew} = \mathrm{tg}^{-1}\,[n\,(532\mathrm{nm})] = \mathrm{tg}^{-1}\,(1.795) = 60.9° \qquad (25)$$

which provides a zero reflectance for polarized light "*p*". The first refracted beam, <1>, has a relative intensity greater than 0.96 and a spectrum very similar to that of the incident beam, even if it shows a slight decrease as the wavelength decreases (see Fig. 23b). So, we can say that the spectrum of the main dispersed beam, <1> of type "*p*", is very similar to that of the input beam. Therefore, in all the experimental cases in which the prism method is still used to measure the spectrum of a white light (modern methods now almost exclusively foresee the use of diffraction gratings), it will be necessary to use the spectral transmissivity function $\mathcal{T}_{P0}(\lambda)\cdot\mathcal{T}_{P1}(\lambda)$, given by Eq. (B.2) of Appendix B, to correct the experimentally measured spectrum. The second refracted beam <2>, not dispersed, shows a spectrum strongly different from that of the incident beam, with an attenuation that increases as the wavelength increases (see Fig. 23c) and tends to zero towards the spectral limit; practically only the violet-blue component of the spectrum is present and the red component is negligible. The beams <3>, <4> and <5> are very similar, from a spectral point of view, to the beam <2> (see Figs. 23d, 23e and 23f), but their relative intensity is progressively lower as the number of internal reflections increases.

To get an overview of the relative spectral intensities of the various beams exiting the prism in polarization "*p*", we report all the intensities in (%) on a logarithmic scale in Fig. 23g. The logarithmic scale is necessary to let all the curves enter in the same graph. It can be seen that the trend of the spectral intensity of the beams from <2> to <5> is very similar. Finally, Fig. 23h shows the cumulative relative intensity of the six beams considered. It can be seen that, after a negligible beam <R>, almost all the intensity of the entrance beam is transferred to the beam <1>, apart from a small portion at the low λ, transferred subsequently to the beam <2>. In conclusion, in polarization "*p*", practically all the incoming light is transferred to the beam <1>.

We now apply the equations reported in Appendix B to the polarization of type "*s*". The "*s*" spectral reflectivity of the prism is quite flat, and therefore the spectrum of the beam <R> is similar to that at input (see Fig. 24a). The transmissivity "*s*" of the beam <1> shows instead a significant increase of the relative intensity at increasing λ, and therefore the spectrum of the beam <1> differs significantly from that at input, especially in the blue-green part, and is less flat than that of polarization "*p*" (see Fig. 24b). Finally, similarly to the polarization "*p*", with the polarization "*s*" the beams from <2> to <5> show a decreasing of the transmissivity with the wavelength (see Figs. 24c-24f), although now the mean relative intensities are higher.

The intensities in (%) on a logarithmic scale of the first six beams exiting the prism, in polarization "*s*", are shown in Fig. 24g. It can be seen how now the intensity of all the bundles is contained within a more reduced logarithmic scale compared to "*p*" polarization. Furthermore, in Fig. 24h the cumulative relative intensity of the six beams considered is reported. It can still be seen how now the beam <R> is no longer negligible, and that the intensity of the inlet beam is distributed mainly on the beams <R>, <1> and <2>.

Now we analyze the spectral behavior of the various beams exiting the prism when the inlet beam is unpolarized. It is sufficient to make the average of the already found components of reflectivity and transmissivity of the "*p*" and "*s*" type. It should be noted, of course, that the beams exiting the prism will all be partially polarized, although the inlet beam it is not. The external reflectivity and the transmissivity of the beams from <1> to <5> are shown in Figs. 25a-25f. The reflected beam has a spectrum very similar to that of the incident beam, apart from a slight attenuation at high λ. The beam <1> too, the main one dispersed, has a spectrum very similar to that of the incident beam, apart from a slight attenuation at low λ. All the other beams instead show a decreasing transmissivity with λ, more or less accentuated. If we compare the dispersed beams, the <1>, <3> and <5>, we find that all three are different from each other and from the entrance beam, but the beam <1> is the most similar to the entrance one. In Fig. 25g the various curves of relative spectral intensity are reported in a single graph in (%) and on a logarithmic scale. As already discussed, the knowledge of the transmissivity relative to the beam <1> makes it possible to make that correction, albeit small, necessary to derive the true spectrum entering the prism, starting from measurements on the beam <1>. Fig. 25h shows the cumulative relative intensity of the first six beams considered.

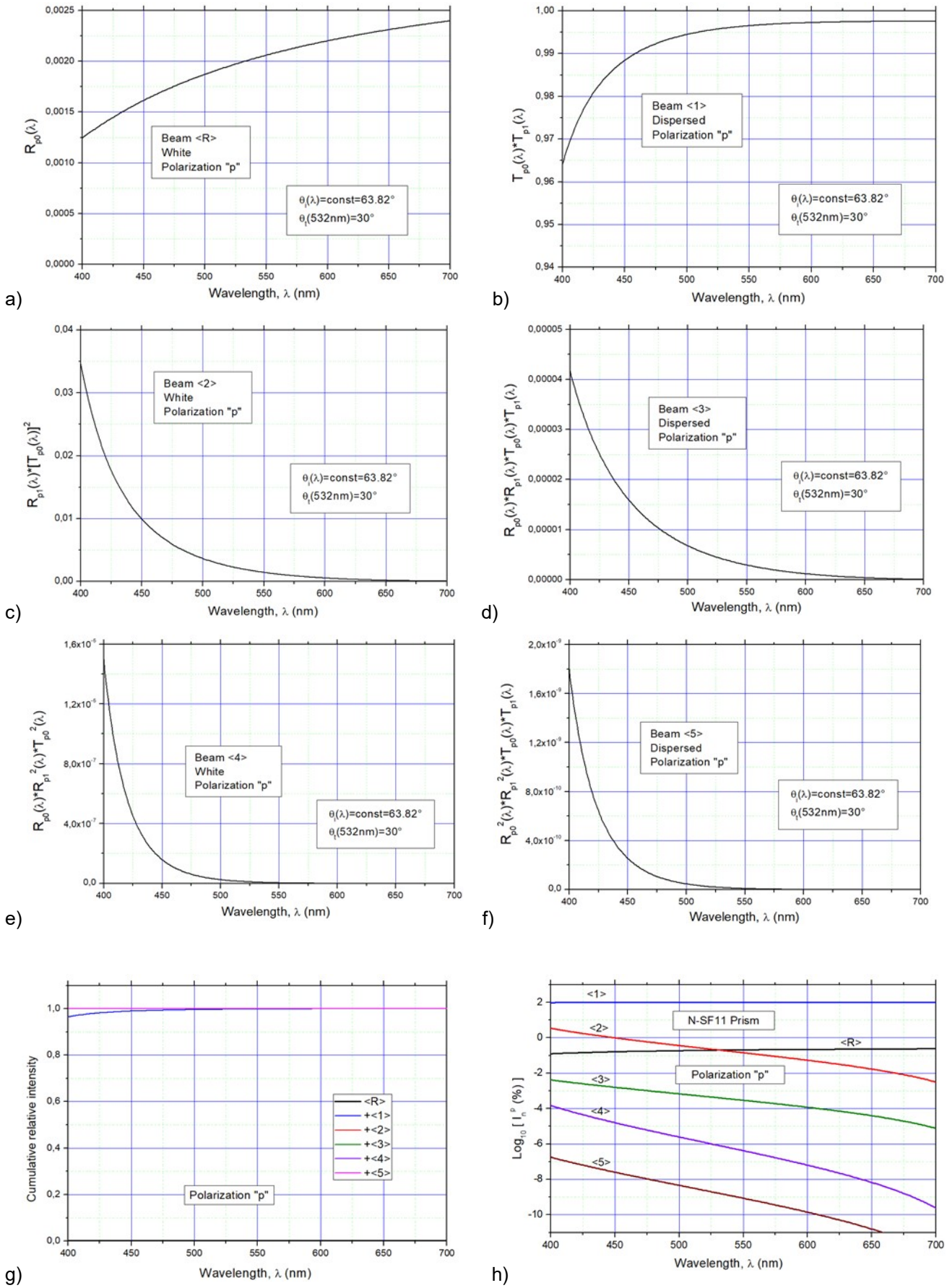

fig. 23. Light "*p*" polarized at input of the prism. (a) Relative spectral reflectivity of beam <R>. (b)-(f) Relative spectral transmissivity of beams <1>-<5>, respectively. (g) Relative spectral intensities (in % on a logarithmic scale) of the first six beams exiting the prism. (h) Cumulative relative spectral intensity of the first six beams exiting the prism.

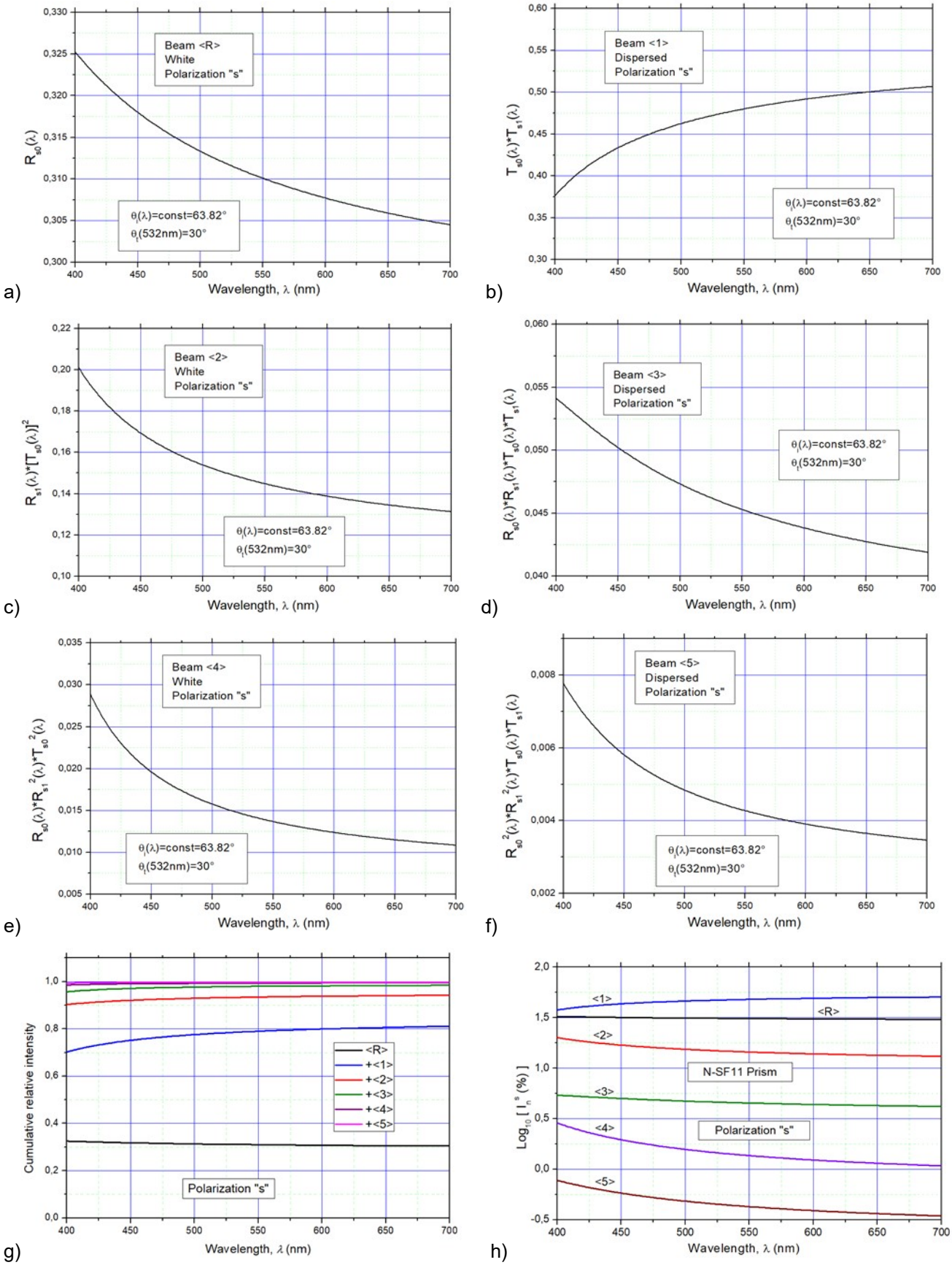

fig. 24. Light "s" polarized at input of the prism. (a) Relative spectral reflectivity of beam <R>. (b)-(f) Relative spectral transmissivity of beams <1>-<5>, respectively. (g) Relative spectral intensities (in % on a logarithmic scale) of the first six beams exiting the prism. (h) Cumulative relative spectral intensity of the first six beams exiting the prism.

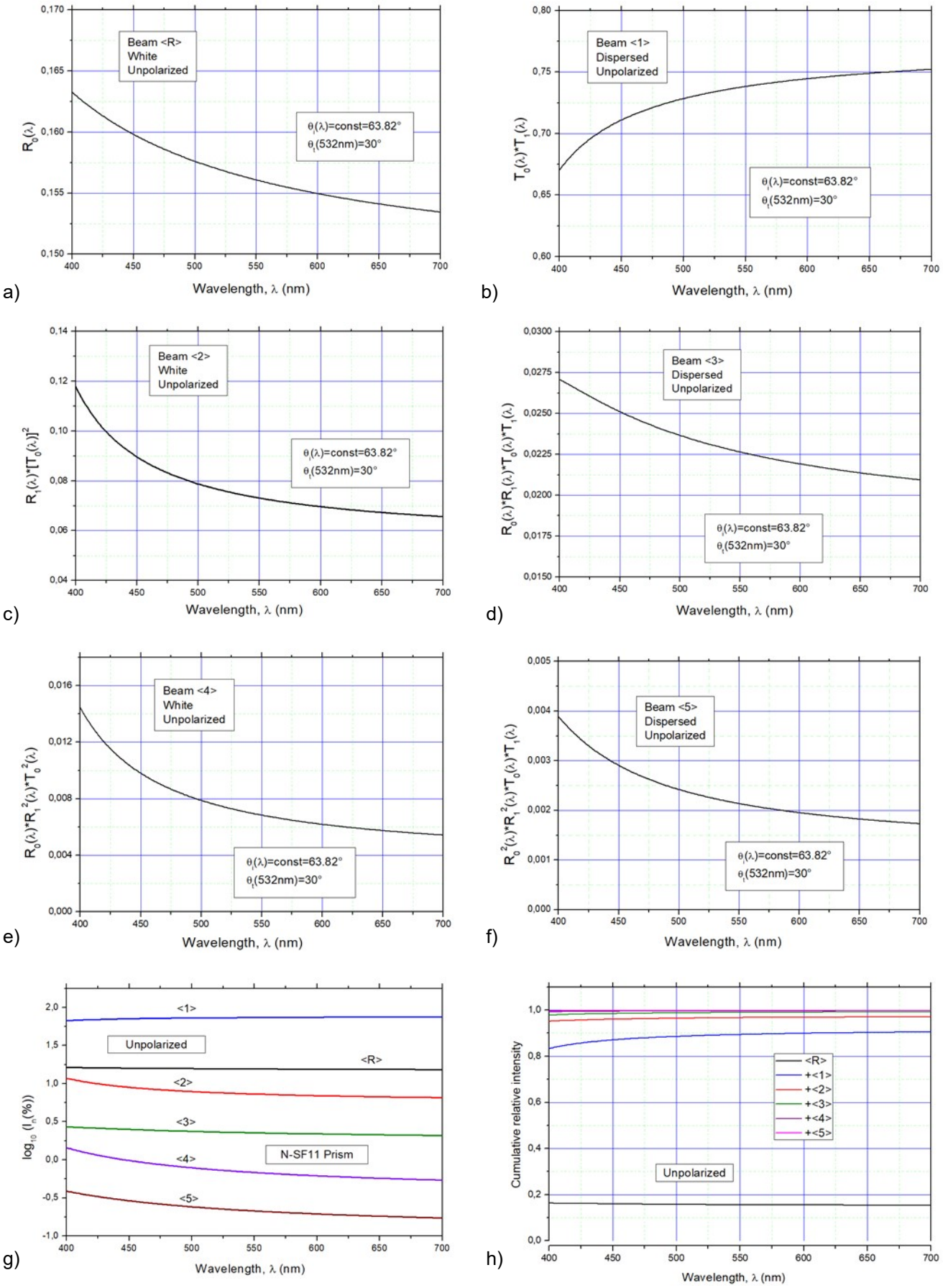

fig. 25. Light unpolarized at input of the prism. (a) Relative spectral reflectivity of beam <R>. (b)-(f) Relative spectral transmissivity of beams <1>-<5>, respectively. (g) Relative spectral intensities (in % on a logarithmic scale) of the first six beams exiting the prism. (h) Cumulative relative spectral intensity of the first six beams exiting the prism.

B. *Exit Angles of the Rays from the Prism*

Let us now calculate the exit angle β_1 from the prism of the first refracted beam <1> as a function of the angle of incidence, β_0, of a white light beam. For the dispersed beams we will examine only the wavelengths: 400nm, 532nm, 632.8nm and 700nm. The white <R> beam naturally has the same exit angle as the entry angle, as well as the white beams <n> with even n, as <2> and <4>, due to the fact that, after an internal reflection, the angles of incidence on the inner wall of the prism are repeated, two by two, and therefore also those refracted externally (see Fig. 26, curve in black).

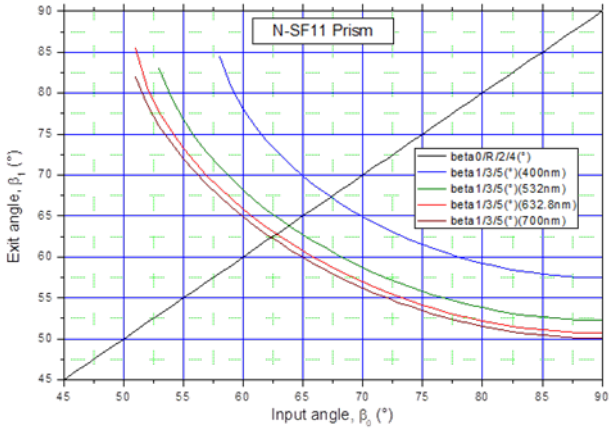

fig. 26. Exit angles of the white beams <R>, <2>, <4> and of the rays at wavelengths: 400nm, 532nm, 632.8nm and 700nm, of the dispersed beams <1>, <3>, <5>, as a function of the angle of incidence of a white beam <0> at input.

The beams <n> with odd n, such as <1>, <3> and <5>, instead, being dispersed, will have different exit angles depending on the wavelength, in particular increasing with decreasing wavelength (see Fig. 26, colored curves); with the same wavelength, however, the exit angles of the beams will be the same for all the values of odd n. For low values of input angle β_0, the beams <1>, <3> and <5> do not appear due to the total internal reflection (TIR). The first to emerge from the TIR condition are the beams <1>, <3> and <5> with λ = 700nm, and then gradually the others at the smaller wavelengths. As can be seen from Fig. 26, the points of intersection of the line of β_1 for n even (line in black), with the curves of β_1 relative to odd n and to different wavelengths (colored curves), identify those values of β_0 for which the rays at the corresponding wavelengths make a symmetrical path within the prism, with internal angles of incidence always equal to 30°. The intersection points move at higher values of β_0 with decreasing wavelength, because, to have the same angle refracted internally at 30°, the angle of incidence at the entrance must be higher for shorter wavelengths, for which the refractive index is higher.

C. *Experimental Measurements with White Light*

The most "suggestive" effects of multiple internal reflections are observed by illuminating the prism with white light. Here we do not make spectral measurements, although they would be of great interest to confirm what is reported in the theoretical Section VI.A, but we will limit ourselves to visualizing on the screens the light emitted by the different faces of the prism. On the other hand, we have already seen the intensity ratio of the different components of refracted light when it is monochromatic, verifying that these calculated ratios agree well with the experimental ones. Fig. 27 shows some photos of the experimental apparatus. The white light of a projector, possibly polarized, is sent to a slit so as to have a line of light that strikes a single face of the prism. Alternatively, the slit is removed to illuminate the prism simultaneously on two faces.

a)

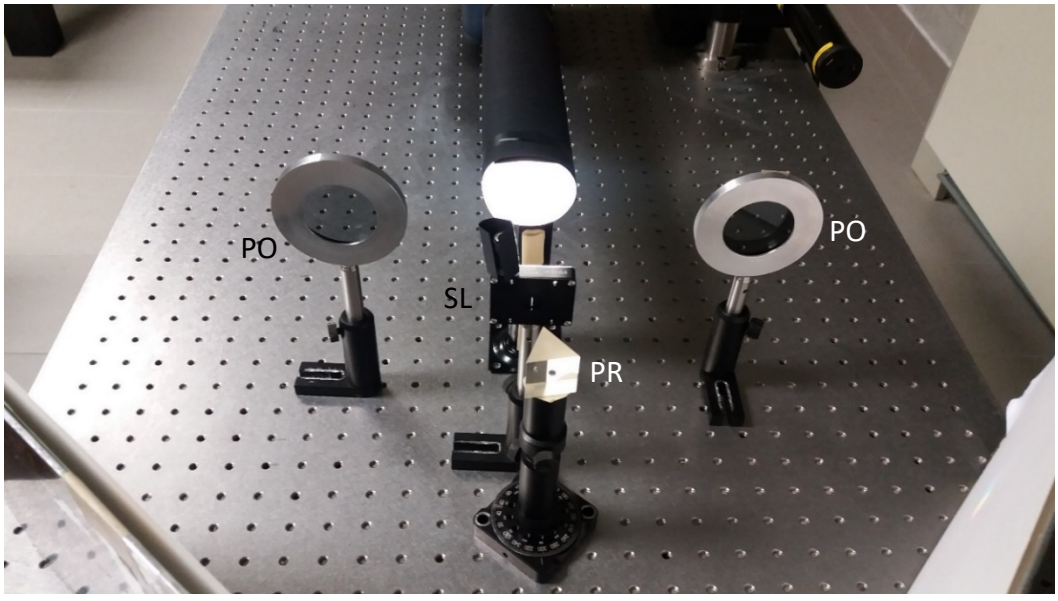

b) 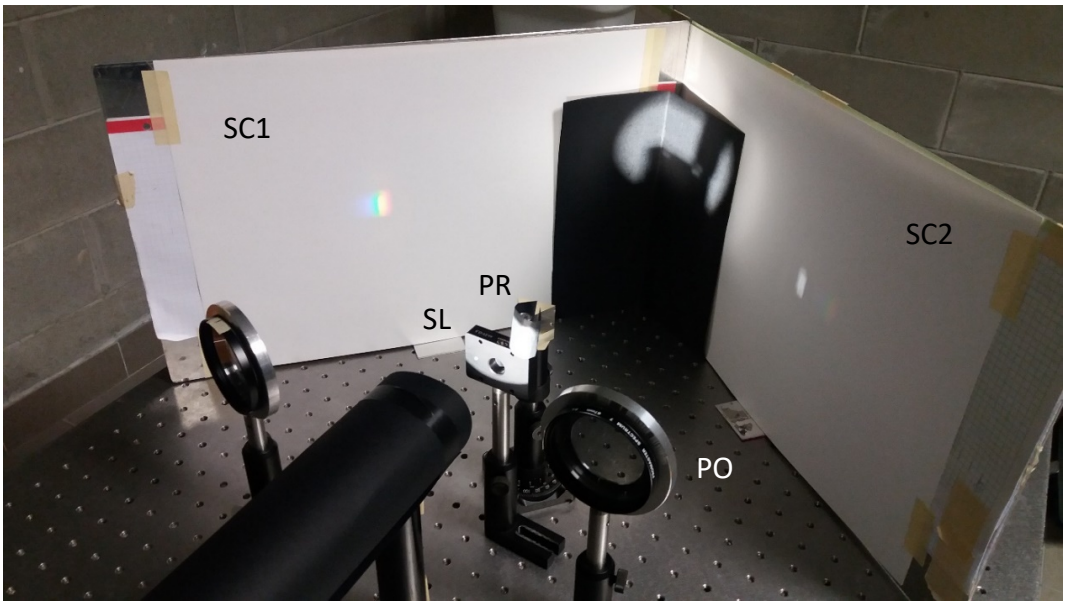

fig. 27. Photos of the experimental apparatus for the visualization of the beams exiting the prism. Legend: PO = polarizer; SL = slit; PR = prism; SC = white screen.

The experimental measurements in white light were limited to the observation of light beams projected on two white screens. We observed the beams in two different conditions. In the first configuration, the light of the lamp was polarized "*p*" or "*s*" and a slit was placed between the polarizer and the prism (see Fig. 27 and 28). In this way, only one face of the prism is illuminated. We were able to observe therefore the beams: <R> white, <1> and <3> dispersed, <4> white (I remember that all the dispersed beams are of odd order, while all the white beams are of even order). The beams <2> and <5> were not observed due to the difficulty in arranging a third screen on the side of the light source. Fig. 28 shows the scheme of the experimental apparatus for visualizing the beams exiting the prism, illuminated through a slit with polarized white light. The prism (PR) is illuminated by the light of the lamp (LP), polarized by the polaroid (PO) and transmitted through the slit (SL). As far as the orientation of the prism with respect to the incident beam is concerned, we know that, by providing an angle of incidence β = 63.8°, we have a symmetrical path with the wavelength of the green light (532nm), which involves the overlapping of all outgoing beams, dispersed and white, considering that green is a central wavelength with respect to the white spectrum. To avoid this, the prism was oriented at ~60° to have β <63.8° (see the scheme at the top of Fig. 28), which involves having β' (532nm) > 63.8° (see Fig. 7), for which we will have a slight separation between the outgoing white beams at β'~60° and the outgoing dispersed beams at β' (λ) > 63.8°. Fig. 28 shows two different orientations of the prism with respect to the incident beam, that is with β ~ 60° (top scheme) and β' > 63.8° (bottom scheme), in which the beams of the two pairs <R> + <3> and <1> + <4> exchange their place. Fig. 29 shows a photo of the screens (SC1) and (SC2) on which the pairs of beams <R> + <3> and <1> + <4> in polarization "*s*" are projected. In the inset, the pair <1> + <4> is shown in the condition in which β < 63.8° and the beam <4> stays side by side with the red color (see the orientation in the upper scheme of Fig. 28). Both in polarization "*p*" and "*s*" the beam <1> was very intense, and therefore, to better visualize or to take photos of it together with the beam <4>, it was necessary to project it on a black screen (see the inset in Fig. 29).

In the second experimental configuration (see Fig. 30), the prism was illuminated on two faces with unpolarized light, having set β = 60°. Because of this configuration, we will have that the light inside the prism will travel partly clockwise and partly counter clockwise. The beams projected on the two screens, identical and visible, will be: <R>, <1>, <3>, <4>, whereas the beams <2> and <5>, projected towards the light source were not observed. Being β ~ 60°, on the two screens we will have the overlapping of the beams <R> and <4>, which appear as a single central white beam, and on the opposite sides the beams <1> and <3> dispersed, with the opposite colors and the red color adjacent to the white beam (a situation that remembers the appearance of the first and second order in rainbows!). Fig. 31 shows the photo of the two screens with the beams projected above and it is possible to distinguish the black background used to attenuate the very intense beam <1>. The inset shows, in particular, a nice photo of the projection area on SC2.

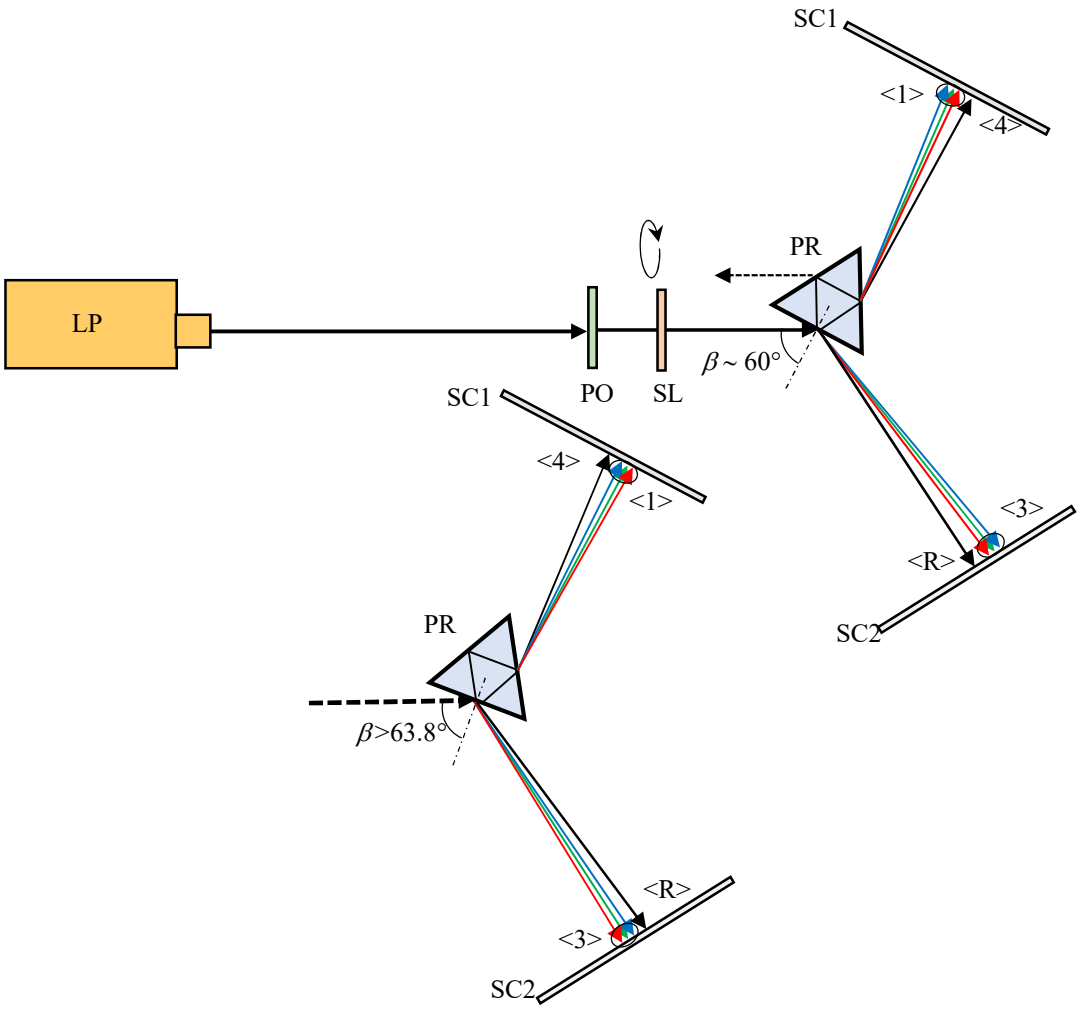

fig. 28. Schematics of the experimental apparatus for visualizing the beams exiting the prism, illuminated in white light through a slit and polarized. The light travels counter clockwise inside the prism. Legend: LP = lamp; PO = polarizer; SL = slit; PR = N-SF11 prism; SC = white screen.

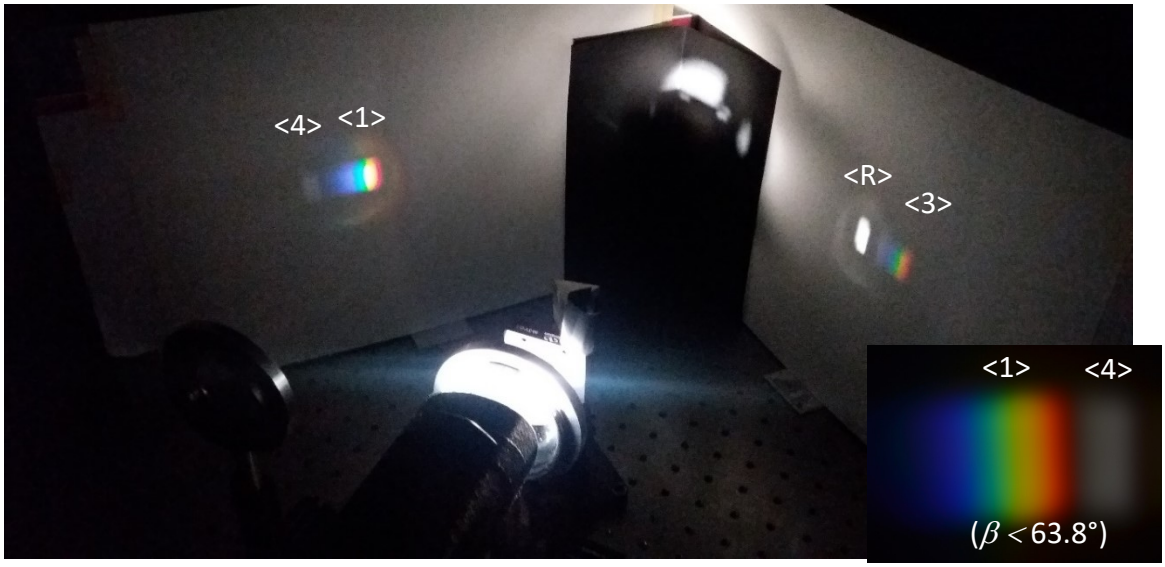

fig. 29. Photo of the two screens on which the pairs of beams <R> + <3> and <1> + <4> are projected, in polarization "s". The inset shows the pair of bundles <1> + <4> when the angle of incidence is β <63.8°.

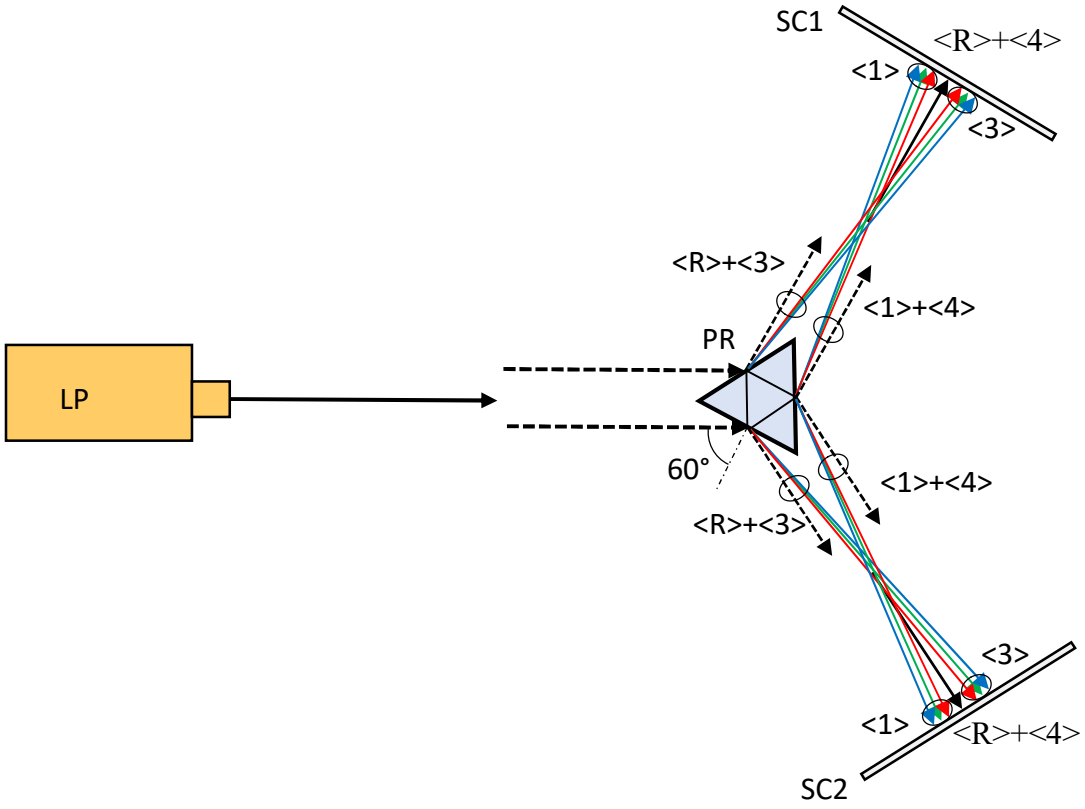

fig. 30. Experimental scheme for the visualization of the beams exiting the prism illuminated on two faces with unpolarized white light. Legend: LP = lamp; PR = prism; SC = screen.

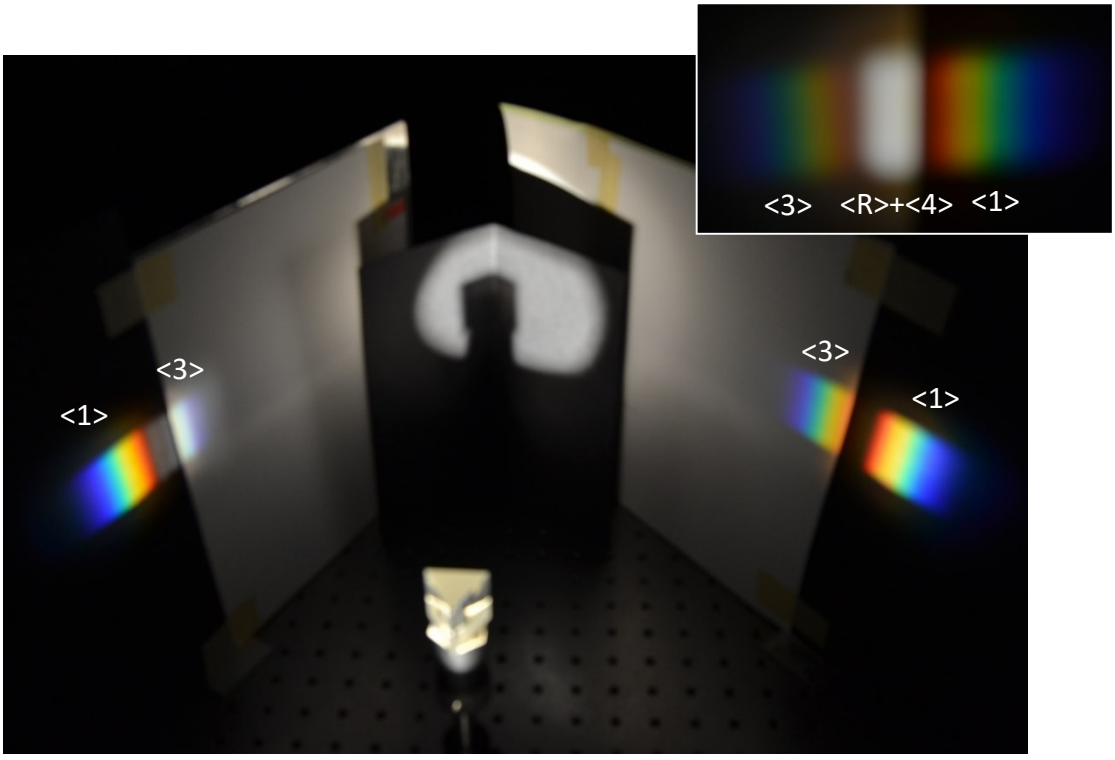

fig. 31. Projection of the beams on the screens when the prism is illuminated on two faces with unpolarized light. The most intense beams are projected on a black screen. The inset shows the photo of the projection area on SC2.

VII. Conclusions

After a brief introduction on the basic concepts of the use of a prism as the optical element capable to produce the spectral dispersion of a white light beam, attention was paid to the particular properties of the equilateral prism by studying the properties of light emitted by the prism as an effect of the multiple internal reflections, when it is illuminated by monochromatic or white light. The optical effects have been multiple, suggestive and didactically very interesting. Illuminating the prism with laser light it was possible to observe up to six externally refracted beams, of which five were subjected to measurement. Polarizing then the incident laser light, the independence between the "*p*" and "*s*" polarization states was observed experimentally. Independence is broken only in particular cases in which the output signal is very low, and is due to a non-perfect alignment between polarizer and prism. Repeatedly applying the Fresnel equations, the intensities of the "*p*" and "*s*" components of the outgoing beams were calculated for monochromatic light, from the reflected beam to the fifth refracted one, which were then compared with the experimentally measured intensities. The agreement was very good, within the experimental errors. Working in white light, we observed a suggestive phenomenon, namely that the light emitted by the faces of the prism consisted of a series of dispersed and white beams, which alternate as a result of the multiple internal reflections, thanks to the geometry of the equilateral prism. This phenomenon is simply due to the fact that the angles of incidence of a ray of light within an equilateral prism can be only two, complementary to 60°. Applying again the Fresnel equations, the spectral transmissivity relative to the first six beams coming out of the prism (the reflected beam and the first five refracted beam) was calculated, for the two polarizations "*p*" and "*s*". It has been also found that all the beams coming out of the prism, white or dispersed, had a spectrum different than the incident beam, but the reflected and the first refracted beams are very similar to the incident one, especially when the incoming light is polarized "*p*" or unpolarized. By virtue of the particular geometry of the equilateral prism, the angular spectral dispersion is exactly the same for all the dispersed beams. Finally, it should be noted that the processing carried out for the calculation of the spectral intensities, and the experiments carried out, have all been referred to a SCHOTT's N-SF11 equilateral prism and to a particular experimental condition, i.e. a symmetrical path inside the prism of the green ray with λ = 532nm. The theoretical treatments carried out in Appendices A and B allow, however, to extend the reported results to any other experimental condition.

VIII. Appendix A. Calculation of Intensities in Mono-chromatic Light

We define the following quantities:

I_0 = intensity of the incident beam;

I_0^p = component *"p"* intensity of incident beam;

I_0^s = component *"s"* intensity of incident beam;

I_n = intensity of output beam <n>;

I_n^p = component *"p"* intensity of output beam <n>;

I_n^s = component *"s"* intensity of output beam <n>;

I_R = intensity of reflected beam <R>;

I_R^p = component *"p"* intensity of reflected beam <R>;

I_R^s = component *"s"* intensity of reflected beam <R>;

T = transmission matrix;

T_n = transmission matrix of output beam <n>;

T_R = transmission matrix of reflected beam <R>;

T_n^p = *"p"* component transmissivity of output beam <n>;

T_n^s = *"s"* component transmissivity of output beam <n>;

T_R^p = *"p"* component transmissivity of reflected beam <R>;

T_R^s = *"s"* component transmissivity of reflected beam <R>.

We have:

$$I_n^p = T_n^p \cdot I_0^p \quad \text{(A.1)}$$

$$I_n^s = T_n^s \cdot I_0^s \quad \text{(A.2)}$$

$$I_R^p = T_R^p \cdot I_0^p \quad \text{(A.3)}$$

$$I_R^s = T_R^s \cdot I_0^s \quad \text{(A.4)}$$

$$I_0 = \begin{pmatrix} I_0^p \\ I_0^s \end{pmatrix} \quad \text{(A.5)}$$

$$I_n = \begin{pmatrix} I_n^p \\ I_n^s \end{pmatrix} = T_n \cdot I_0 \quad \text{(A.6)}$$

$$I_R = \begin{pmatrix} I_R^p \\ I_R^s \end{pmatrix} = T_R \cdot I_0 \quad \text{(A.7)}$$

If the alignment between the beam and the prism is correct, T_n and T_R must be diagonal matrices:

$$T_n = \begin{pmatrix} T_n^p & 0 \\ 0 & T_n^s \end{pmatrix}; \; T_R = \begin{pmatrix} T_R^p & 0 \\ 0 & T_R^s \end{pmatrix} \quad \text{(A.8)}$$

And then:

$$I_n = \begin{pmatrix} T_n^p & 0 \\ 0 & T_n^s \end{pmatrix} \cdot \begin{pmatrix} I_0^p \\ I_0^s \end{pmatrix}; \quad I_R = \begin{pmatrix} T_R^p & 0 \\ 0 & T_R^s \end{pmatrix} \cdot \begin{pmatrix} I_0^p \\ I_0^s \end{pmatrix} \tag{A.9}$$

The intensities of the beams exiting from the prism have been calculated starting from the Fresnel equations [29]. The light reflectivity $\mathcal{R}$ and light transmissivity $\mathcal{T}$ through the air/glass or glass/air interface, in correspondence to the *"p"* and *"s"* polarizations, are given by:

$$\mathcal{R}_p = \frac{\tan^2(\theta_i - \theta_t)}{\tan^2(\theta_i + \theta_t)} \tag{A.10}$$

$$\mathcal{T}_p = \frac{\sin(2\theta_i)\cdot\sin(2\theta_t)}{\sin^2(\theta_i + \theta_t)\cdot\cos^2(\theta_i - \theta_t)} \tag{A.11}$$

$$\mathcal{R}_s = \frac{\sin^2(\theta_i - \theta_t)}{\sin^2(\theta_i + \theta_t)} \tag{A.12}$$

$$\mathcal{T}_s = \frac{\sin(2\theta_i)\cdot\sin(2\theta_t)}{\sin^2(\theta_i + \theta_t)} \tag{A.13}$$

Let us consider a symmetrical path for the passage from air to glass of the green (532 nm) ray at input; we have:

$$\theta_i = \sin^{-1}\left[n\cdot\sin\theta_t\right] = \sin^{-1}\left[n\cdot\sin(30°)\right] = \ldots$$
$$\ldots = \sin^{-1}\left[1.7948\cdot 0.5\right] = 63.82° \tag{A.14}$$

The angles θ_i and θ_t will be exchanged when considering the passage from glass to air. From Fresnel Eqs. (A.10)–(A.13), we observe that all the trigonometric functions are symmetrical with respect to the angles of incidence and transmission, i.e. they do not change if the passage takes place between air/glass or glass/air. Given then for the intensity of the incident beam at input I_0 = 1, the intensity of the various beams, reflected or refracted, becomes:

$$I_R^p = \mathcal{R}_p\ ; \quad I_1^p = \mathcal{T}_p^2\ ; \quad I_2^p = \mathcal{R}_p\cdot\mathcal{T}_p^2; \quad I_3^p = \mathcal{R}_p^2\cdot\mathcal{T}_p^2\ ;$$
$$I_4^p = \mathcal{R}_p^3\cdot\mathcal{T}_p^2\ ; \quad I_5^p = \mathcal{R}_p^4\cdot\mathcal{T}_p^2\ ; \ldots \tag{A.15}$$

$$I_R^s = \mathcal{R}_s\ ; \quad I_1^s = \mathcal{T}_s^2\ ; \quad I_2^s = \mathcal{R}_s\cdot\mathcal{T}_s^2\ ; \quad I_3^s = \mathcal{R}_s^2\cdot\mathcal{T}_s^2\ ; \quad I_4^s$$
$$= \mathcal{R}_s^3\cdot\mathcal{T}_s^2\ ; \quad I_5^s = \mathcal{R}_s^4\cdot\mathcal{T}_s^2\ ; \ldots \tag{A.16}$$

For the refracted beams, we can then write the following compact formulas:

$$I_n^p = \mathcal{R}_p^{n-1}\cdot\mathcal{T}_p^2\ ; \quad I_n^s = \mathcal{R}_s^{n-1}\cdot\mathcal{T}_s^2 \tag{A.17}$$

IX. Appendix B. Calculation of Intensities in Polychro-matic Light

Since we are now dealing with non-monochromatic light, we cannot apply the formulas (A.15) - (A.17), which are valid only for λ = 532 nm. In the case of polychromatic light, the transmission angle at the first refraction, $\theta_{t0}(\lambda)$, will be different from the angle of incidence at the second refraction, $\theta_{t1}(\lambda) = 60° - \theta_{t0}(\lambda)$, therefore, in the case, for example, of *"p"* polarization, we must distinguish the component $\mathcal{T}_p$ at the first refraction, which we will call $\mathcal{T}_{p0}$, from that at the second refraction, which we will call $\mathcal{T}_{p1}$; in the subsequent refractions, the $\mathcal{T}_p$ components will return to being equal to those relating to two previous refractions, i.e.: $\mathcal{T}_{p2} = \mathcal{T}_{p0}$; $\mathcal{T}_{p3} = \mathcal{T}_{p1}$; $\mathcal{T}_{p4} = \mathcal{T}_{p0}$; $\mathcal{T}_{p5} = \mathcal{T}_{p1}$; and so on. A similar argument applies to the reflectivity $\mathcal{R}$: $\mathcal{R}_{p2} = \mathcal{R}_{p0}$; $\mathcal{R}_{p3} = \mathcal{R}_{p1}$; $\mathcal{R}_{p4} = \mathcal{R}_{p0}$; $\mathcal{R}_{p5} = \mathcal{R}_{p1}$; and so on.
We will have, therefore, in the case of *"p"* polarization:

$$I_R^p(\lambda) = I_0^p(\lambda)\cdot\mathcal{R}_{p0}[\theta_{i0}, \theta_{t0}(\lambda)]; \tag{B.1}$$

$$I_1^p(\lambda) = I_0^p(\lambda)\cdot\mathcal{T}_{p0}[\theta_{i0}, \theta_{t0}(\lambda)]\cdot\mathcal{T}_{p1}[\theta_{i1}(\lambda), \theta_{t1}(\lambda)]; \tag{B.2}$$

Being:

$$\theta_{i0} = const = \sin^{-1}[n(532nm)\cdot 0.5] = 63.8° \tag{B.3}$$

$$\theta_{i0}(\lambda) = \sin^{-1}[\sin(\theta_{i0})/n(\lambda)] \tag{B.4}$$

$$\theta_{i1}(\lambda) = 60° - \theta_{t0}(\lambda) \tag{B.5}$$

$$\theta_{t1}(\lambda) = \sin^{-1}[\sin(\theta_{i1}(\lambda))\cdot n(\lambda)] \tag{B.6}$$

$$I_2^p(\lambda) = I_0^p(\lambda)\cdot\mathcal{R}_{p1}[\theta_{i1}(\lambda), \theta_{t1}(\lambda)]\cdot\ldots$$
$$\ldots\cdot\{\mathcal{T}_{p0}(\theta_{i0}, \theta_{t0}(\lambda))\}^2 \tag{B.7}$$

$$I_3^p(\lambda) = I_0^p(\lambda)\cdot\mathcal{R}_{p1}[\theta_{i1}(\lambda), \theta_{t1}(\lambda)]\cdot\ldots$$
$$\ldots\cdot\mathcal{R}_{p2}[\theta_{i0}(\lambda), \theta_{t0}(\lambda)]\cdot\mathcal{T}_{p0}[\theta_{i0}, \theta_{t0}(\lambda)]\cdot\ldots$$
$$\ldots\cdot\mathcal{T}_{p1}[\theta_{i1}(\lambda), \theta_{t1}(\lambda)] \tag{B.8}$$

$$I_4^p(\lambda) = I_0^p(\lambda)\cdot\{\mathcal{R}_{p1}[\theta_{i1}(\lambda), \theta_{t1}(\lambda)]\}^2\cdot\ldots$$
$$\ldots\cdot\mathcal{R}_{p2}[\theta_{i0}(\lambda), \theta_{t0}(\lambda)]\cdot\{\mathcal{T}_{p0}[\theta_{i0}, \theta_{t0}(\lambda)]\}^2 \tag{B.9}$$

$$I_5^p(\lambda) = I_0^p(\lambda)\cdot\{\mathcal{R}_{p1}[\theta_{i1}(\lambda), \theta_{t1}(\lambda)]\}^2\cdot\ldots$$
$$\ldots\cdot\{\mathcal{R}_{p2}[\theta_{i0}(\lambda), \theta_{t0}(\lambda)]\}^2\cdot\mathcal{T}_{p0}[\theta_{i0}, \theta_{t0}(\lambda)]\cdot\ldots$$
$$\ldots\cdot\mathcal{T}_{p1}[\theta_{i1}(\lambda), \theta_{t1}(\lambda)] \tag{B.10}$$

Similar equations apply for the *"s"* polarization.

ACKNOWLEDGEMENT

The author thanks very much Prof. Roberto Calabrese, of the Department of Physics and Earth Sciences of the Ferrara University, for having promoted this type of experiments, which were carried out at his own Optical Laboratory.

REFERENCES

[1] D. Park, The Fire Within the Eye, Princeton University Press, Princeton, New Jersey, U.S.A., 1997, pp. 221-226.

[2] T. G. Kyle, Atmospheric Transmission, Emission and Scattering, Pergamon Press, Oxford, U.K., 1991, pp. 91-97.

[3] J. R. Meyer-Arendt, Introduzione all'Ottica Classica e Moderna, Zanichelli, Bologna, I., 1976, pp. 80-82.

[4] F. J. Dijksterhuis, "Understandings of colors: varieties of theories in the color worlds of the early seventeenth century", Early Science and Medicine, 20 (2015) 515-535.

[5] S. D. Gedzelman, M. Vollmer, "Progress in atmospheric optics and light and color in nature", Bull. of the American Meteorological Society, 90 (2009) 689-693.

[6] R. Stothers, "Ancient meteorological optics", The Classical Journal, 105 (2009) 27-42.

[7] S. D. Gedzelman, M. Vollmer, "Atmospheric optical phenomena and radiative transfer", Bull. of the American Meteorological Society, 89 (2008) 471-485.

[8] P. Johnson, "Proof of the heavenly iris: the fountain of three rainbows at Wilton House, Wiltshire", Garden History, 35 (2007) 51-67.

[9] P. Hughes-Hallett, "The Mystery of the rainbow", New England Review, 23 (2002) 131-145.

[10] G. Hoffmann, Newton's Prism Experiment and Goethe's Objections. http://docs-hoffmann.de/prism16072005.pdf.

[11] M. J. Riedl, Optics for Technicians, SPIE Press, London, U. K., 2015.

[12] W. Neumann, Fundamentals of Dispersive Optical Spectroscopy Systems, SPIE Press, Lewiston, NY, U.S.A., 2014.

[13] M. Born and E. Wolf, Principles of Optics, Cambridge University Press, Cambridge, UK, 2011, pp. 190-193.

[14] D. Park, The Fire Within the Eye, Princeton University Press, Princeton, New jersey, 1997, 197-205.

[15] D. S. Loshin, The Geometrical Optics Workbook, Butterworth-Heinemann, Mishawaka, IN, U.S.A. 1991.

[16] A. A. Mills, Newton's Prisms and His Experiments on the Spectrum, Royal Society, London, U.K., 1981.

[17] G. S. Landsberg, Ottica, Edizioni MIR, Mosca, 1979, pp. 311-313.

[18] J. R. Meyer-Arendt, Introduzione all'Ottica Classica e Moderna, Zanichelli, Bologna, 1976, pp. 72-79.

[19] R. Kingslake, Applied Optics and Optical Engineering, Vol. V, Part II, Optical Instruments, Academic Press, New York, 1969, pp. 1-16, 48-52.

[20] I. Newton, Opticks (Royal Society, London, 1704), Dover Publications, Inc., New York, 1952, p. 20.

[21] A. E. Shapiro, "Experiment and mathematics in Newton's theory of color", Phys. Today 37 (Sept. 1984) 34–42.

[22] https://refractiveindex.info/

[23] M. Born and E. Wolf, Principles of Optics, (Cambridge University Press, Cambridge, UK) 1999, p. 49-54.

[24] F. S. Crawford, "Variations on a famous white-light experiment of Isaac Newton", Am. J. Phys. 39, (Dec. 1971) 1538-1539.

[25] T. Greenslade Jr., "Spectrum recombination", The Physics Teacher, 22 (Feb. 1984) 105-108.

[26] A. Guillemin, Les Phenomenes de la Physique, Libraire de L. Hachetteet Cie, Paris, 1868, p.353.

[27] D. Brewster, Memoirs of the Life, Writings, and Discoveries of Sir Isaac Newton, Vol. I, Thomas Constable and Co., 1855.

[28] S. Grusche, "Revealing the nature of the final image in Newton's experimentum crucis", Am. J. Phys. 83 (July 2015) 583–589.

[29] M. Born and E. Wolf, Principles of Optics, Cambridge University Press, Cambridge, UK, 2011, pp. 40-49.

[30] A. Parretta, Optical Methods for the Characterization of PV Solar Concentrators, Chapter 13, pp. 316-416, in: Advances in Optics: Reviews. Book Series, Vol. 3. Ed. by Sergey Y. Yurish. Published by International Frequency Sensor Association (IFSA) Publishing, S. L., 2018. ISBN: 978-84-697-9439-5.

[31] E. Bonfiglioli, Sviluppo di Metodi per la Caratterizzazione Ottica Indoor di Concentratori Solari, Graduate Thesis in Physics and Astrophysics, Università degli Studi di Ferrara, A. A. 2007-2008, Ferrara, Italy.